Downcoast Redistribution of Changjiang Diluted Water due to Typhoon Chan-Hom (2015)

Yunpeng Lin[1], Yunhai Li[2], Shuai Cong[3], Meng Liu[1], Liang Wang[2], Binxin Zheng[2], and Jingping Xu[1]

[1]Southern University of Science and Technology
[2]Third Institute of Oceanography, Ministry of Natural Resources
[3]Ocean University of China, China.

March 6, 2023

Abstract

Typhoons are known to substantially influence the coastal circulation and the associated biogeochemical processes. The transport of Changjiang Diluted Water (CDW), an important source to the coastal current in the East China Sea (ECS), varies markedly under the influence of typhoons. This study quantitively details the downcoast transport of CDW driven by Typhoon Chan-Hom in the summer of 2015. Salinity measurements 3 days after the typhoon's passage showed the presence of a large volume of low salinity water, up to 70 km wide and 20 m thick along the Zhejiang-Fujian coastal area with an estimated freshwater volume of 3.7×1010 m3. A three-endmember mixing model shows that the CDW's contribution to the study area's surface waters (<10 m) immediately after the typhoon was as high as 40% (average 32%), much greater than the contribution under normal summer conditions of 8% (average 3%). The vast spreading of CDW along the Zhejiang-Fujian coast created a strong stratification in the upper water column that limited the diffusion of CDW in the study area. The calculated and observed results suggest that these abnormal low salinity water could stay in the study area for 13-21 days. Additional nutrients in the CDW elevated the Chlorophyll-a concentration in the upper water column (mean 3.74 mg m-3) and produced large amount of particulate organic carbon (POC).

Hosted file

957277_0_art_file_10744507_rqs60s.docx available at https://authorea.com/users/443412/articles/627609-downcoast-redistribution-of-changjiang-diluted-water-due-to-typhoon-chan-hom-2015

Downcoast Redistribution of Changjiang Diluted Water due to Typhoon Chan-Hom (2015)

Yunpeng Lin[1], Yunhai Li[2, 3*], Shuai Cong[4], Meng Liu[1], Liang Wang[3], Binxin Zheng[3], Jingping Xu[1, 2*]

[1]Department of Ocean Science & Engineering, Southern University of Science and Technology, China.

[2]Laboratory for Marine Geology, Qingdao National Laboratory for Marine Science and Technology, China.

[3]Third Institute of Oceanography, Ministry of Natural Resources, China.

[4]College of Marine Geosciences, Key Laboratory of Submarine Geosciences and Prospecting Techniques, Ocean University of China, China.

Corresponding author: Yunhai Li (liyunhai@tio.org.cn), Jingping Xu (xujp@sustech.edu.cn)

Key Points:

- Typhoon Chan-Hom caused an alongshore strip of low salinity water strip, up to 70 km wide and 20 m thick, along the Zhejiang-Fujian coast.
- Up to 40% (32% average) of this low salinity water strip was sourced from Chanjiang Diluted Water (CDW).
- The long residence time (13-21 days) of this low salinity and eutrophic water elevated the Chlorophyll-a concentration in the upper water column.

Abstract

Typhoons are known to substantially influence the coastal circulation and the associated biogeochemical processes. The transport of Changjiang Diluted Water (CDW), an important source to the coastal current in the East China Sea (ECS), varies markedly under the influence of typhoons. This study quantitively details the downcoast transport of CDW driven by Typhoon Chan-Hom in the summer of 2015. Salinity measurements 3 days after the typhoon's passage showed the presence of a large volume of low salinity water, up to 70 km wide and 20 m thick along the Zhejiang-Fujian coastal area with an estimated freshwater volume of 3.7×10^{10} m^3. A three-endmember mixing model shows that the CDW's contribution to the study area's surface waters (<10 m) immediately after the typhoon was as high as 40% (average 32%), much greater than the contribution under normal summer conditions of 8% (average 3%). The vast spreading of CDW along the Zhejiang-Fujian coast created a strong stratification in the upper water column that limited the diffusion of CDW in the study area. The calculated and observed results suggest that these abnormal low salinity water could stay in the study area for 13-21 days. Additional nutrients in the CDW elevated the Chlorophyll-a concentration in the upper water column (mean 3.74 mg m^{-3}) and produced large amount of particulate organic carbon (POC).

Plain Language Summary

In normal summer conditions, the Changjiang Diluted Water (CDW) mainly expands offshore to the northeast toward the Tushima Strait. When typhoons strike the area, however, the downcoast transport of CDW was enhanced so much that its contribution to the water along Zhejiang-Fujian costal area grows 10-folds from 3% to as much as 30%. These typhoon induced low salinity water float above the high salinity continental shelf water and can stay in the Zhejiang-Fujian costal area for 13-21 days. Nutrients brought by the CDW increase the pramiry productivity in

the surface water with much higher concentration of Chrolophyll-a and particulate organic carbon.

1 Introduction

The Changjiang (Yangtze) River is the most important sources of freshwater and terrestrial materials to the continental shelf of the East China Sea (ECS) (Beardsley et al., 1985; Chang and Isobe, 2003; Yang et al., 2014), responsible for 66% and 84% of the annual nitrogen and phosphorus input into the eastern coastal area around China, respectively (Tong et al., 2015). The Changjiang Diluted Water (CDW) is one of the major drivers to render significant impacts on the circulation system, ecological environment and sedimentary geomorphology of the eastern shelf seas of China, especially the Yellow and East China Seas (Chai et al., 2006; Li et al., 2002; Li et al., 2014; Wu et al., 2013; Wu and Wu, 2018; Zhou et al., 2008). In the normal winter conditions, the downcoast Zhejiang-Fujian Coastal Current (ZFCC) is an important branch of CDW propagation on the ECS (Figure 1a) that the fresh discharge can reach 1.5×10^4 m^3 s^{-1}, which is comparable to the Changjiang River runoff in the same season, and the total water discharge can reach 2×10^5 m^3 s^{-1} (Wu et al., 2013). In summer, the CDW expands offshore to the northeast in the form of a jet stream that can go as far as the Tsushima Strait and the Korean Strait driven primarily by the southerly monsoon wind (Lie et al., 2003; Shang et al., 2009; Lee et al., 2017; Hou et al., 2021).

Previous studies showed that the main dynamic controls on the CDW expansion described above include Changjiang River runoff, sea surface wind, offshore current and tidal circulation (Beardsley et al., 1985; Chang and Isobe, 2003; Lee et al., 2017; Wu et al., 2013; Wu and Wu, 2018). However, the above mentioned "normal" seasonal patterns can be easily altered by short time-scale weather events such as typhoons, whose extreme wind can change the regional circulation entirely for a short period of time (Hou et al., 2021; Lee et al., 2017; Wu et al., 2021; Zhang et al., 2018). Additionally, high surface waves during typhoons enhance the mixing of the upper water column that can lead to the reinforcement of the buoyant coastal currents (Zhang et al., 2018). Numerical modeling results have shown that typhoon induced vertical mixing of the water column not only significantly inhibits and delays the CDW extension toward Jeju Island for up to 20 days (Lee et al., 2017), but also helps to form a stronger buoyant coastal current that propagates downcoast toward 27°N, a coastal circulation pattern normally seen in winter (Zhang et al., 2018). The downcoast freshwater transport due to Typhoon Chan-Hom accounted for 53% of Changjiang River runoff in the same period, or 5% of the total runoff in 2015 (Zhang et al., 2018). Given the fact that there are on average 2-4 typhoons passing through the region every year (Su 2005; Chen et al., 2017), the transport of CDW (or freshwater) by the coastal currents toward the Zhejiang-Fujian coast and its impact to the shelf ecosystem of the region cannot be ignored. Large phytoplankton blooms and enhanced primary productivity in the typhoon-affected area, either due to nutrient input from freshwater (Li et al., 2013; Wang et al., 2017) or the vertical mixing upwelling that transport the bottom water with high nutrients to the surface (Lin et al., 2003; Pana et al., 2017; Li et al., 2022) have been observed. For example, remote sensing results showed that Typhoon Chan-Hom triggered dramatic increase of Chlorophyll-a in the ECS, which was construed as typhoon-induced upwelling (Li et al., 2022) and downcoast transported CDW supporting (Zhang et al., 2018), respectively. In addition to nutrients, typhoon-driven water transport (including riverine diluted water) is likely to facilitate transport, accumulation and deposition of terrestrial particulate materials, such as sediment and particulate organic matter (POM) (He et al., 2014).

Most, if not all, of these findings are the results from various modeling studies. Due to lack of field data (because of extreme difficulties of conducting field work during typhoon), they could only be validated against remote sensing data (Zhang et al., 2018; Li et al., 2022) that are limited to the sea surface. Here we present the results from an investigation that was specifically designed to fill this data gap, and it is of great significance to deeply understand the physical-biogeochemical synergies in ECS during typhoon. In the remaining sections of the manuscript, the geological and hydrodynamical settings of the study area and the Typhoon Chan-Hom are introduced first, followed by a brief description of the methods used in collecting and analyzing the data and samples. Section 4 presents the key findings of the study, and section 5 attempts to address the following inquiries through a thorough discussion of the results: the volume and residence time of CDW brought to the study area by Typhoon Chan-Hom and the ecological impact of this extra CDW. Section 6 concludes.

2 Regional setting

2.1 Study area

The study area is located about 430 km southwest of the Changjiang River Estuary, part of the inner shelf of the ECS off the rugged coastline of Zhejiang and Fujian Provinces (Figure 1a). The tide in the region is mainly the regular semi-diurnal tide with average tidal ranges of 4-5 meters for during spring tide and 2-3 meters during neap. Two current systems dominate the regional shelf circulation: the nearshore Zhejiang-Fujian Coastal Current (ZFCC) and the offshore Taiwan Warm Current (TWC) (Figure 1a). While the TWC flows upcoast all year round (Zhu et al., 2004), the ZFCC flows upcoast in summer but downcoast in winter, primarily controlled by the wind directions of the East Asia monsoons (Jan et al., 2002; Wu et al., 2013).

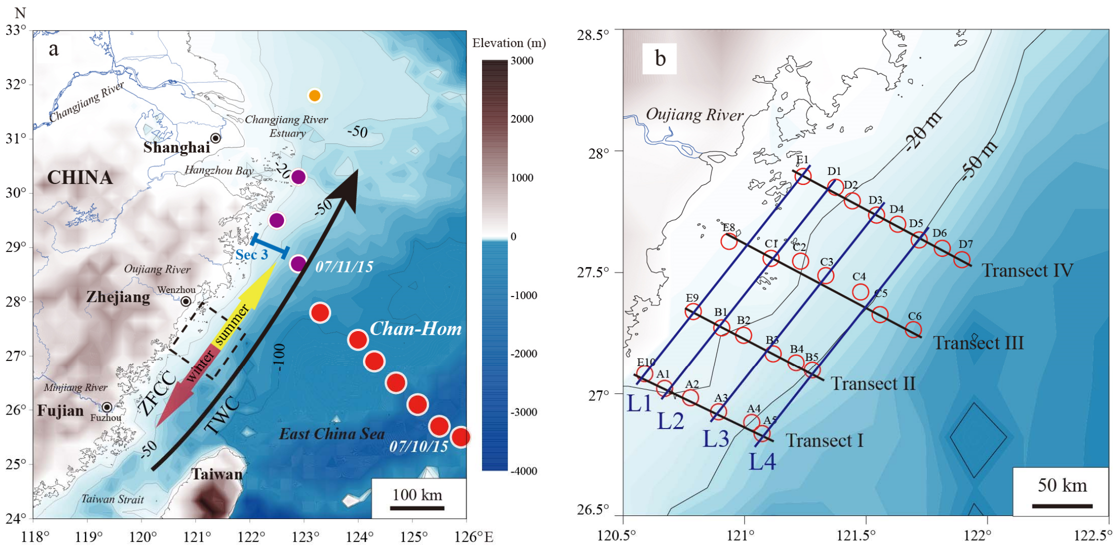

Figure 1. (a) The track of Typhoon Chan-Hom in July 10 to 11 2015 (modified from the typhoon track data at http://typhoon.weather.com.cn/) and location of study area. The colored dots indicate the typhoon center with the size and color indicating the categories of typhoon: the red dots represent a category of Super Typhoon with wind speed of > 51 m s^{-1}; the purple dots represent a category of strong Typhoon with wind speed of 42-51 m s^{-1}; the orange dot represent a category of Typhoon with wind speed of 32-41 m s^{-1}. The red and yellow arrows represent Zhejiang-Fujian Coastal Current (ZFCC) in winter and summer, respectively (Jan et al., 2002; Wu et al., 2013), whereas the black arrow represents Taiwan Warm Current (TWC) (Zhu et al., 2004). The transect in blue color (Sec 3) was the position where freshwater discharge was calculated by Zhang et al. (2018). (b) Station locations and survey transects. The red circles indicate stations set in the post-typhoon and normal conditions. The black lines indicate the

cross-shelf transects (I, II, III, and IV) and blue lines indicate the along-shelf transects (L1, L2, L3, and L4).

2.2 Typhoon Chan-Hom

After forming in the western Pacific on 30 June 2015, Typhoon Chan-Hom headed northwest toward the coast of Zhejiang. It grew into a super typhoon on 10 July while entering the ECS. By the time, Chan-Hom arrived at the shallow water just northeast of study area on July 11, its maximum wind speed reached 58 m s^{-1} with the air pressure of 925 hPa. The radius of Grade 7 and 10 (13.9 and 24.5 m s^{-1}, respectively) wind circles were as large as 460 and 180 km. Chan-Hom landed near the Changjiang River Estuary on 16:40 (UTC+8) July 11, 2015 (Figure 1a), and turned northeastward back into the Yellow Sea and gradually dissipated.

3 Data and Methods

3.1 Data recordings and water sample collections

This study aims to capture typhoon's impact, so the field work was designed to have two cruises: one immediately after typhoon's passing (and sea conditions permitting) representing post-typhoon oceanographic condition, and another about 3 weeks after the typhoon representing the 'normal' oceanographic environment. The post-typhoon survey was conducted 14-15 July and the second survey was carried out later on 4-5 August. It took roughly 36 hours to complete each survey during which CTD (conductivity-temperature-depth, SD204) cast was performed at each of the 27 stations that constituted four cross-shore transects (Figure 1b). In addition to vertical profiles of water temperature, salinity, and depth that were recorded by the CTD at a sampling rate of 1 Hz, Chlorophyll-a concentration were also collected with a fluorometer

(SEAPOINT) mounted on the CTD frame. The fluorometer was also set to sample at 1 Hz with a detection range of 0 to 10 mg m^{-3}. At each station, water samples were collected in the CTD's rosette bottles that were triggered at six regularly-spaced depths (0, 0.2, 0.4, 0.6, 0.8, 1.0 of local water depth) during each CTD cast. For safety reasons, the CTD was kept from hitting the seabed so the bottom samples were actually from 1-2 m above the seafloor.

Auxiliary data such as regional winds and sea surface currents during Typhoon Chan-Hom were download from online public domain. The 10 m wind field data was obtained from the reanalysis product of ERA5-Interim (http://apps.ecmwf.int/datasets/data/mediate_full_daily/) of the European Centre for Medium-Range Weather Forecasts (ECMWF). The sea surface current data was obtained from the French Copernicus Marine Environment Monitoring Service (CMEMS) (http://marine.copernicus.eu/). The spatial resolution both the download wind and sea surface current data is 0.5°× 0.5°.

3.2 Laboratory sample analyses

The water samples from each station were divided into two parts. The first part was filtered through pre-weighed double acetate membranes with a diameter of 47 mm (pore size of 0.45 μm) for suspended paticulate matter (SPM) measuement, which were rinsed with distilled water to remove the salt and dried at 40°C, and then weighed using an electronic balance with a precision of 10^{-5} g. The second part, used for particulate organic carbon (POC), particulate nitrogen (PN), and $\delta^{13}C$ estimation, was filtered through all-glass-fiber Whatman GF/F membrane of 47 mm diameter and 0.7 μm pore size that were pre-cauterized at 450°C for 6 h. After drying in a 40℃ oven for 12 hours, the glass filters were acid-steamed in a closed container with concentrated hydrochloric acid for 12 h for carbonates removal. Those filters were then dried again in a 60℃ oven. A special puncher was used to take a small piece of known surface area of the membrane and the then wrapped in a tin cup. The POC and δ^{13}C of samples were measured by Elemental Analyzer - Stable Isotope Mass Spectrometer (EA-IRMS, Integra 2, SerCon, UK). The instruments were first run with three blank samples, and two standard samples were also run between every 12 field samples. Because both the filtered water volume and the ratio of the punched/whole surface area of the membrane are known, the total mass of carbon on the whole membrane and the volume concentration of POC can be readily calculated. The δ^{13}C value is based on VPDB (Vienna Pee Dee Belemnite) international standard as a reference standard. The analytical accuracy was ±0.5% for POC, ±0.4% for PN, and ±0.2‰ for δ^{13}C.

The δ^{13}C values were calculated as:

$$\delta = \left(\frac{(^{13}C/^{12}C)_{sample}}{(^{13}C/^{12}C)_{standard}} - 1\right) \times 1000 \qquad (1)$$

3.3 mixing model

A three-endmember mixing model (Wang et al., 2017) was used in this study to calculate the contributions of Changjiang Diluted Water (CDW), shelf surface water (SSW), and shelf bottom water (SBW) to the water in study area. A Monte Carlo (MC) Simulation strategy was applied to track the source distribution of water masses with the consideration of the spread end-member parameter values (Andersson, 2011). The program was run in Enthought Python Distribution 7.2, and the code was provided by Li et al. (2012a). Basically, 400, 000 out of 40,000,000 random samples from the normal distribution of each end-member were taken in order to simultaneously fulfill the equations:

$$T_{CDW}f_{CDW} + T_{SSW}f_{SSW} + T_{SBW}f_{SBW} = T_{sample} \qquad (2)$$

$$S_{CDW}f_{CDW} + S_{SSW}f_{SSW} + S_{SBW}f_{SBW} = S_{sample} \qquad (3)$$

$$f_{CDW} + f_{SSW} + f_{SBW} = 1 \qquad (4)$$

where T and S are temperature and salinity, respectively, and f is the fraction of each endmember. All temperatures and salinities in Equations 2 – 4 must be known (Table 1) in order to solve the three unknown fractions. T_{sample} and S_{sample} are in-situ values recorded during the CTD cast. The temperature and salinity values of the CDW endmember are from Wang et al. (2017). The average measured values of temperature and salinity recorded during the 'normal' condition survey from station D7, which is farthest from shore and at the deepest water among all CTD stations (Figure 1), were used as the shelf water endmember: with surface water (<10 m) representing the SSW and bottom water (66-76 m) representing the SBW. The contribution of each endmember was calculated based on these 400,000 results. The mean, minimum, and maximum values and standard deviation of each sample in both surveys were showed in the Tables S1 and S2. The mean values were chosen as the final results.

Table 1. End-member characteristics of water masses.

Water mass	T (℃)	S (psu)
CDW*	28.13±0.70	11.54±1.45
SSW	28.90±0.59	33.89±0.05
SBW	17.64±0.01	34.70±0.01

*Reported by Wang et al. (2017).

3.4 Numerical modeling

An Unstructured Grid, Finite-Volume Community Ocean Model (FVCOM) (Chen et al., 2003, 2006) was also utilized to investigate the variation of residual currents in the cross-shelf and along-shelf direction under the impact of Typhoon Chan-Hom. The model domain contains the entire ECS, Yellow and Bohai Seas, with the horizontal resolution of the mesh varied from ~1-3 km near the Zhejiang-Fujian coast to around 10-20 km at the open boundary (Cong et al., 2021). In order to capture ocean response to synoptic wind events, the hourly sea surface forcing data was derived from the National Center for Environmental Prediction (NCEP) Climate Forecast System Version 2 (CFSv2, spatial resolution 0.205°×0.204°) (Saha et al., 2011), which produced wind field well agreed with the observations during Typhoon Chan-Hom (Chu et al., 2019).

The model was validated with multiple observational datasets under normal weather conditions as well as during Typhoon Chan-Hom (Cong et al., 2021). And the model results overall well matched the observational data from different sources as the root-mean-square deviation (RMSD) values of variables are less than 0.8, and the correlation coefficients are high up to >0.83 (More detailed could be seen in Cong et al., 2021). Overall, it presents a satisfying performance for simulating the regional ocean dynamic processes, especially under the impact of Chan-Hom (Cong et al., 2021).

4 Results

4.1 Temperature and salinity structure in the post-typhoon and normal conditions

Figure 2 plots the along-transect profiles of temperature, salinity, and density compiled respectively using CTD data from the two surveys, representing post-typhoon state (hereafter PTS) and normal condition state (hereafter NCS). The entire water column was 1-3 ℃ cooler in PTS than in NCS (Figure 2a). Thermoclines were present on the surface layer in both states, but PTS showed much stronger vertical gradients. On the sea surface, inshore water was warmer than off-shore for PTS. But the opposite is true for the NCS – offshore surface water was warmer than inshore. The mid-layer of water column showed temperature uniformity in PTS, but there was a significant seaward gradient in NCS. The low temperature water invaded along the seabed in the bottom layer of transects III and IV was more extensive in PST than NCS (Figure 2a). Interestingly, the depth of thermocline (about 10 m) was shallower than the halocline (about 20 m) in PTS, and there was not a halocline in NCS. The water salinity in the PTS was significantly decreased in the surface water with a lowest salinity of 25.02 psu (Table 2, Figure 2b). This low saline water (salinity <30 psu) was distributed in a ~70 km wide and ~20 m thick shoreline-parallel strip (Figure 2b). The high temperature and low salinity of surface water reveal a significant stratification in the water column post-typhoon, resulting in a significant pycnocline (Figure 2c), which was similar to the halocline.

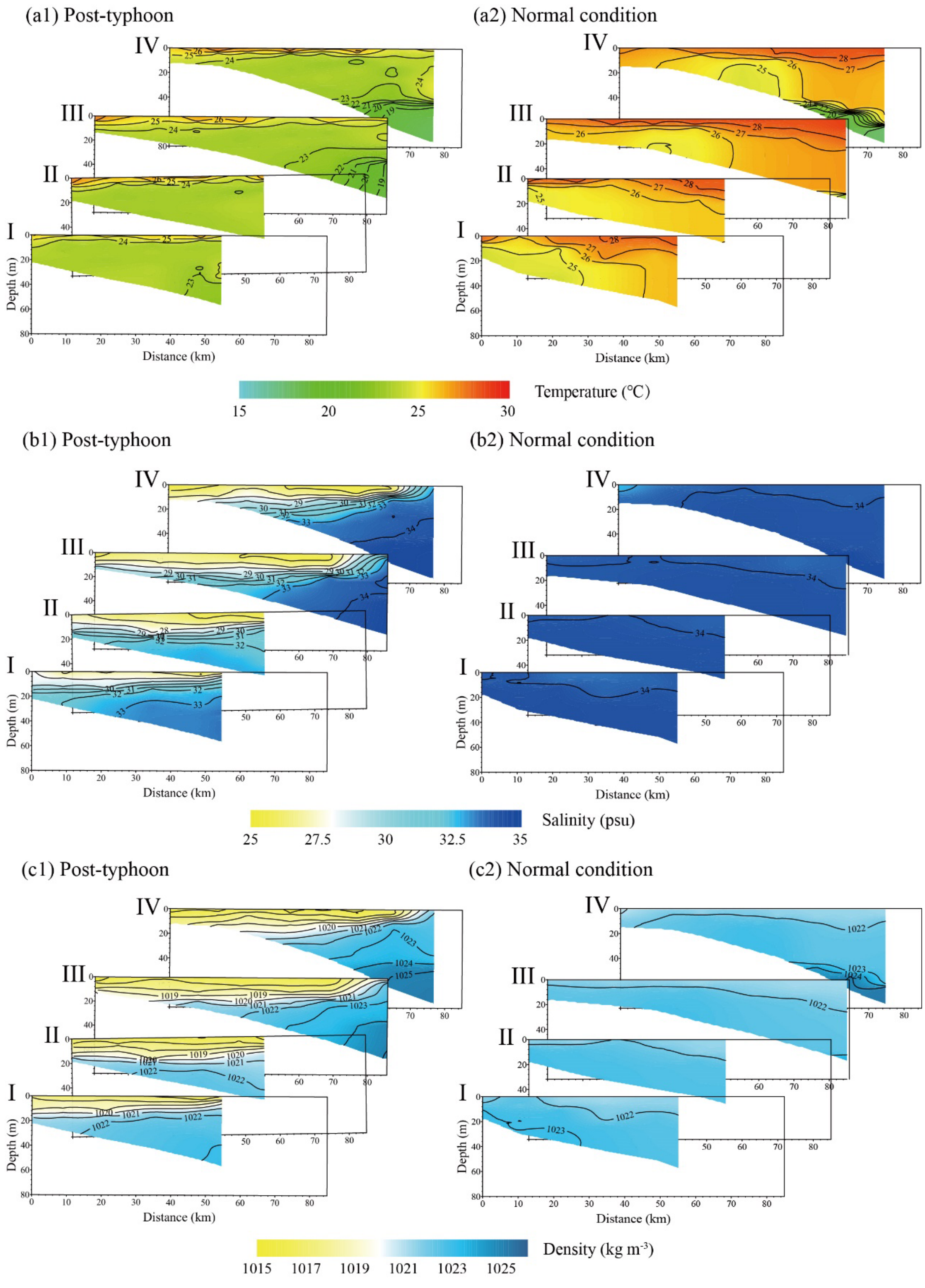
(a1) Post-typhoon
(a2) Normal condition
Temperature (°C)
15 20 25 30
(b1) Post-typhoon
(b2) Normal condition
Salinity (psu)
25 27.5 30 32.5 35
(c1) Post-typhoon
(c2) Normal condition
Density (kg m⁻³)
1015 1017 1019 1021 1023 1025
Depth (m)
Distance (km)
IV
III
II
I

242

Figure 2. The measured water (a) temperature, (b) salinity, and (c) density along 4 cross-shelf transects immediately after the passing of Typhoon Chan-Hom (left panels) and 3 weeks later (right panels).

Table 2. Different parameter of water column in the study area in the post-typhoon and normal conditions. Numbers in parentheses are average values.

Parameters	Post-typhoon		Normal condition	
	Surface (<10m)	Whole column	Surface (<10m)	Whole column
Temperature (℃)	22.83-27.81 (24.53)	18.12-27.81 (23.17)	24.64-28.91 (27.23)	17.64-28.91 (25.91)
Salinity (psu)	25.02-33.49 (27.56)	25.02-34.66 (31.23)	32.66-34.22 (33.87)	32.66-34.55 (34.1)
Chl-a (mg m^{-3})	0.42-29.53 (3.74)	0-29.53) (1.25)	0.03-2.81 (0.5)	0.03-2.96 (0.46)
POC (mg L^{-1})	0.09-0.85 (0.30)	0.06-0.87 (0.25)	0.05-0.47 (0.18)	0.05-0.63 (0.20)
PN (mg L^{-1})	0.025-0.164 (0.071)	0.017-0.182 (0.059)	0.008-0.093 (0.035)	0.008-0.095 (0.037)
$\delta^{13}C$ (‰)	-26.4 - -16.2 (-21.8)	-26.6 - -16.2 (-22.6)	-26.2 - -19.3 (-22.6)	-26.9 - -18.0 (-22.8)
POC (mg L^{-1})	8.4-35.8 (16.9)	8.4-376.3 (29.3)	0.5-31.7 (7.7)	0.3-130.5 (13.2)

4.2 Distribution of Chlorophyll-a, POC, PN, and $\delta^{13}C$

Chlorophyll-a is one of the important indicators of marine primary productivity (Hung et al., 2011; Liu et al., 2018). In PTS, the Chlorophyll-a concentration in the water ranged from 0.13 to 29.53 mg m^{-3} with an average of 1.25 mg m^{-3}. The high Chlorophyll-a values were distinctively limited in the near-surface water roughly above the pycnocline (Table 2, Figure 3, a1), indicating a elevated marine primary productivity in the surface layer. Chlorophyll-a in the NCS was much lower, ranging from 0.03 to 2.96 mg m^{-3} (average of 0.46 mg m^{-3}). Several high value blobs (still much smaller than PTS highs) occurred rather randomly in the water column of the 4 transects (Figure 3, a2).

The concentration of suspended POC in the water column and its isotopic composition ($\delta^{13}C$) are important indicators of marine biogeochemical process (Gao et al., 2014). The concentrations of POC and PN were listed in Table 2. The high POC was occurred in the surface water (Table 2), but it was discontinuous horizontally (Figure 3, b1). The distribution of PN was similar to POC, thus it was not shown here. The $\delta^{13}C$ value of POC range from -26.6 to -16.2 ‰ (averaged -22.6‰). Both the values of POC concentration and $\delta^{13}C$ were lower in the NCS than that in the PTS (Table 2). In the PTS, the $\delta^{13}C$ value showed a significant vertical decrease without obvious seaward variation, and the distribution of high values were consistent with the higher POC concentration (Figure 3, c1). In contrast, strong vertical mixing and obvious seaward decrease occurred in the NCS (Figure 3, c2), similar to the results in the southern ECS reported by Liu et al. (2018). The lower $\delta^{13}C$ (< 25‰) mainly occurred in the offshore region, which may be influenced by the oligotrophic TWC origned from Kuroshio Subsurface Water with low $\delta^{13}C$ from -31 to -27 ‰ (Wu et al., 2003).

272 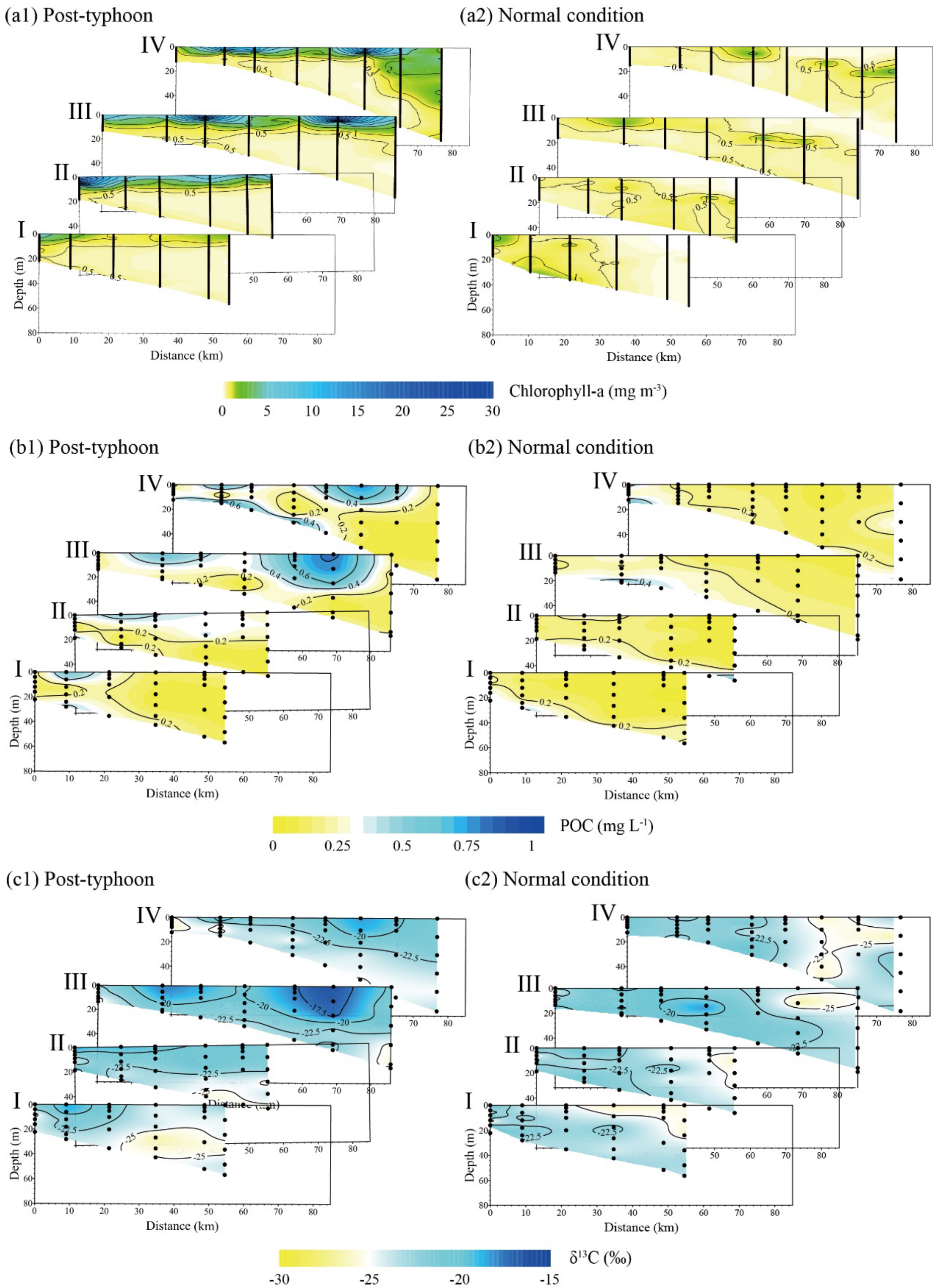
(a1) Post-typhoon
(a2) Normal condition
(b1) Post-typhoon
(b2) Normal condition
(c1) Post-typhoon
(c2) Normal condition
IV
III
II
I
Depth (m)
Distance (km)
Chlorophyll-a (mg m-3)
POC (mg L-1)
δ13C (‰)

Figure 3. The measured (a) Chlorophyll-a, (b) POC concentration, and (c) δ^{13}C value along 4 cross-shelf transects immediately after the passing of Typhoon Chan-Hom (left panels) and 3 weeks later (right panels).

5. Discussion

5.1 Freshwater sources contributing to the low salinity water

The presence of a large (120 km long, 70 km wide, and 20 m thick) low salinity water (as low as 26 psu, Figure 2b) in the study area are immediately after the typhoon, suggesting that the passage of Typhoon Chan-Hom brought an immense amount of freshwater to the study area. The total volume of freshwater (V_f) can be simply estimated as:

$$V_f = \sum_{j=1}^{4} \sum_{i=1}^{M-1} \sum_{k=1}^{N} \frac{S_0 - S_{i,k}}{S_0} \times h_{i,k} \times \Delta d_i \times \Delta l_j \qquad (5)$$

where $S_{i,k}$ is the water salinity in the k^{th} layer at the i^{th} survey station in cross-shore transect j (j = I, II, III, and IV, Figure 1b); S_0 is the ambient salinity (here was 34); M and N are the number of horizontal sites and vertical layers, respectively; $h_{i,k}$ is the thickness of each layer and Δd_i is the distance between two sites; Δl_j is the alongshore length of transect j. Applying the CTD measured salinities, along with all known values for parameters h, d, and l, the post-typhoon (14 July 2015) V_f reached about 3.7×10^{10} m^3. In the same period, the Changjiang River discharge was only ~5×10^4 m^3 s^{-1} with a daily discharged volume of ~ 4.3×10^9 m^3 (Zhang et al., 2018).

A small river, Oujiang, discharges freshwater directly into the study area, therefore should have influenced the salinity of the area (Li et al., 2012b). Precipitation data showed that there was no significantly change of rainfall (<20 mm, Figure S1) in the drainage basin of the Oujiang

River during Typhoon Chan-Hom's passage (9-12 July), thus the river discharge should be close to 4.6-6.2 × 10^2 m^3 s^{-1}, the average rate under normal condition (Yang and Yin, 2018). Three days of continuous discharge by Oujiang would have contributed 1.2 – 1.6 × 10^6 m^3 freshwater to the study area. Theses volumes are nearly 4 orders of magnitude smaller than the freshwater volume that would be required to form the low salinity water layer. Therefore, the runoff input from the Oujiang River had very limited impact that may be limited to only a few stations near the shore like that occurred in the NCS (Figure 2, b2). The CDW, advanced to the study area during Typhoon Chan-Hom (Wu and Wu, 2018; Zhang et al., 2018), is most likely the freshwater source.

A three-endmembers mixing model was used to quantify the contribution of CDW to the water mass in the study area. The plot of temperature vs. salinity for both surveys (Figure 4) suggest that the water in the study area was regulated by three distinct primary water masses: Changjiang diluted water (CDW), shelf surface water (SSW), and shelf bottom water (SBW). The CDW was formed from Changjiang runoff mixing with coastal seawater, that is characteristically high in temperature and low in salinity (Wang et al., 2017). Both the SSW and SBW are continental shelf water with similar salinity, but the temperature of SSW is significantly higher than that of SBW due to solar heating of the surface water. The continuing mixing of three water masses is also responsible for the gradual salinity increase downcoast.

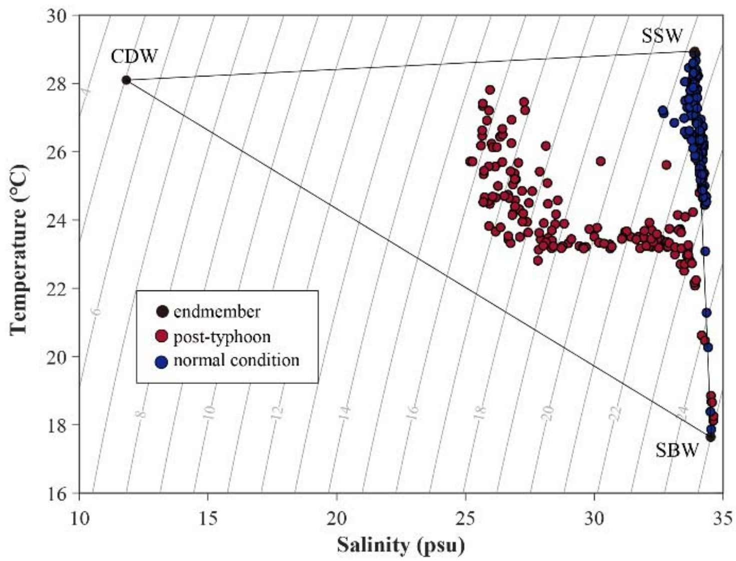

Figure 4. Scatter plot of temperature vs. salinity: post-typhoon condition (red circles) and normal condition (blue circles). The labeled vertices represent the three endmember water masses: Changjiang Diluted Water (CDW), Shelf Surface Water (SSW), and Shelf Bottom Water (SBW). The endmember value of CDW was reported by Wang et al. (2017), and the endmember values of SSW and SBW was average values of surface water (<10 m) and bottom water (66-76 m) collected in the second survey at station D7. The isolines of potential density σ (kg m^{-3}) are shown as gray lines.

The results of mixing model (Table 3) show that the CDW contributed 32% (maximum 40%) to the surface water (<10 m) and 21% to the whole water column in the inner shelf of ECS after Typhoon Chan-Hom (Figure 5). The SSW contributed 40% to the surface water and 40% to the whole water column, and the SBW contributed 29% to the surface water and 39% to the whole water column. However, in the NCS (3 weeks after Typhoon Chan-Hom), the water column was dominated by SSW, perhaps due to the overall shallow water depth in the study area (<50 m), where only several samples below the 50 m water depth were significantly affected by

SBW (Figure 5a). The CDW contributions in the NCS were almost negligible: 3% to the surface water (<10 m) and 2% to the whole water column (Table 3). The distribution of salinity in NCS (Figure 2, b2), which was similar to a typical summer pattern reported by Li et al. (2013), indicates that these contribution of CDW did not come from the residual CDW transported by Typhoon Chan-Hom. There may be two sources of the relative low salinity water in NCS. The first source is Oujiang River runoff, which mainly affected the near-shore station of transect IV and let to a maximum CDW contribution of 8% (Figure 5b). The second source was downcoast transport CDW in the normal summer condition, which has been reported by Wu et al. (2018) using numerical model but still need further investigations. Of course, these results do not affect the thesis of this study for CDW transport induced by typhoon process.

Table 3. Contributions of water masses to the study area in the post-typhoon and normal conditions.

Water masses	Post-typhoon		Normal condition	
	Surface (<10m)	Whole column	Surface (<10m)	Whole column
CDW	32%	21%	3%	2%
SSW	39%	40%	83%	75%
SBW	29%	39%	15%	22%

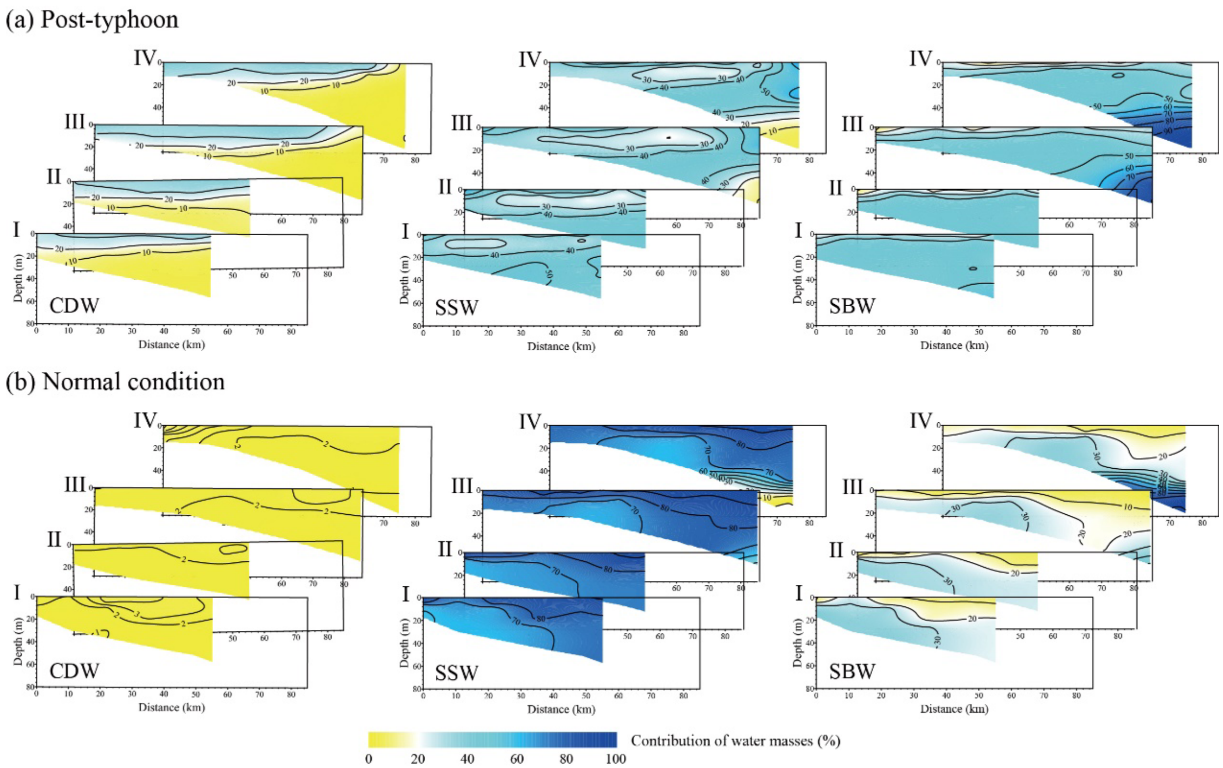

Figure 5. The calculated contribution fraction of Changjiang Diluted Water (CDW, left panels), Shelf Surface Water (SSW, middle panels) and Shelf Bottom Water (SBW, right panels) along 4 cross-shelf transects (a) immediately after the passing of Typhoon Chan-Hom and (b) 3 weeks later.

5.2 Downcoast transport of typhoon-indued CDW

In summer, the prevailing southerly monsoon winds as well as the wind-driven Ekman transport and the northward flowing ZFCC work together to push the CDW offshore and keep the majority of CDW from reaching Zhejiang-Fujian coastal area (Lie et al., 2003; Hou et al., 2021). There have been reports that downcoast transport of CDW driven by buoyant coastal currents under normal summer conditions could reach the northern Zhejiang coastal area (Wu et al., 2018), but that is ~100 km north of sites of this study. This study showed that, under normal summer conditions, the contribution of CDW in the water column along the coast of Zhejiang-Fujian was almost negligible, accounting for only 2%-3% (Table 3, Figure 5b). Under the influence of typhoons, however, significant downcoast transport of CDW elevated the contribution to as high as 30% (Table 3, Figure 5a). Numerical simulations (Zhang et al., 2018) revealed that the downcoast transport of CDW under the influence of Typhoon Chan-Hom was first controlled by typhoon wind-driven currents and then by buoyant coastal currents maintained by surface wave-induced mixing. Across the transect south of the Changjiang River Estuary (29°N, shown in Figure 1a), the downcoast discharge of freshwater can reach ~7×10^4 m^3 s^{-1} with a total duration of up to nearly 10 days (Zhang et al., 2018). This discharge had far exceeded the freshwater transported downcoast by the ZFCC in winter (1.5×10^4 m^3 s^{-1} in the same transect reported by Wu et al., 2013) and even exceeded the Changjiang River runoff in summer (~5×10^4 m^3 s^{-1}) (Zhang et al., 2018), which also indicates that the downcoast transport of CDW under typhoon influence was not only from the direct input of the Changjiang River runoff, but also included a large volume of CDW that originally stayed in the offshore area of the Changjiang River Estuary.

To clarify Typhoon Chan-Hom's impact on the water discharge into the study area, we re-run the FVCOM (Cong et al., 2021) to compute the hourly residual current crossing the four cross-shelf survey transects (I, II, III, and IV) and four along-shelf transects (L1, L2, L3, and L4, see Figure 1b), which allowed us to calculate the time variation of water discharge (Q) in both the alongshore and cross-shore directions:

$$Q_{transect} = \sum_{i=1}^{M-1}\sum_{k=1}^{N} v_{i,k} \times h_{i,k} \times \Delta d_i \tag{6}$$

where $v_{i,k}$ is daily average along-shore (or cross-shore) velocity of current in the k^{th} layer at the i^{th} survey station. All other parameters are the same as in Equation 5.

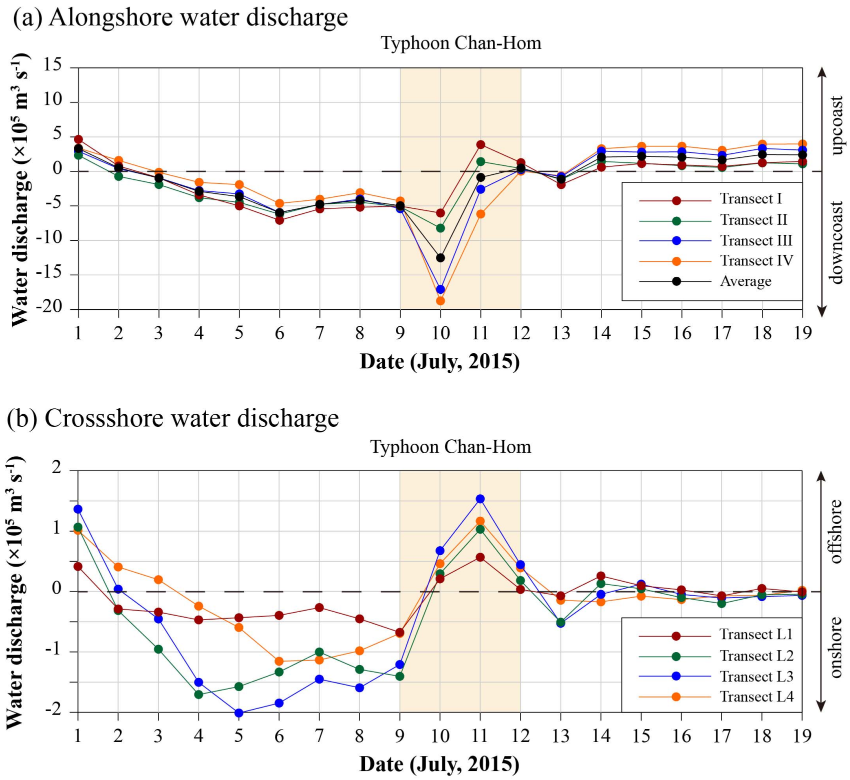

Figure 6. The calculated (a) along-shore and (b) cross-shore water discharge during 1 July to 19 July, 2015. Positive values are upcoast or offshore direction.

Figure 6 plots the time-series of water transport across the alongshore and cross-shore transects. Under normal condition (1-2 July), there was upcoast water transport in the study area, which was controlled by typical summer ZFCC (Yanagi et al., 1996; Wu et al., 2013). Prior to the typhoon landfall (3-9, July), a steady downcoast transport (~5×10^5 m^3 s^{-1}, Figure 6a) was present for several days. The pattern is consistent with findings in another study (Zhang et al., 2018), even though their cross-shelf transect (Sec 3 in Figure 1a) is about 200 km northeast of this study area. The steady northerly wind at the front of the typhoon's wind field (Figure 7, a1-

a2) during this time was responsible for the persistent downcoast transport. During Typhoon Chan-Hom (10-11, July), the downcoast discharge of the water in the study area was greatly enhanced 2-3 folds (~15×10^5 m^3 s^{-1}, Figure 6a), and there was a significant gradient with the distance from the typhoon center, especially on 11 July (Figure 6a). The wind and current fields shifting back to a typical summer pattern (predominantly southerly winds and the northeastward ZFCC) south of the study area are likely the cause (Figure 7, a3-a4 and b3-b4). The downcoast water transport weakened rapidly, even reversed to upcoast direction when Typhoon Chan-Hom passed the area, but a smaller downcoast transport returned on July 13, driven by the buoyant coastal currents, but only lasted for one day (Figure 6a). By July 14, the whole study area was fully returned to typical summer southerly winds and northeastward wind-driven current (Figure 7, a7 and b7). Because this upcoast transport was on average only 16% of the typhoon induced downcoast transport (Figure 6a), a large volume of CDW still remained in the surface waters of Zhejiang-Fujian coastal area 3-4 days after the Typhoon Chan-Hom (Figure 5a). The cross-shore water transport (Figure 7b) in the study area was first directed onshore, and then off-shore during Typhoon Chan-Hom (Figure 6b and Figure 7). The cross-shore water transport significantly decreased after the typhoon, nearly 1 order of magnitude smaller than the alongshore counterpart. The cross-shore water transport in the study area was clearly controlled by the wind-driven Ekman transport under the impact of Typhoon Chan-Hom. It took only 3-4 days for the typhoon's effect on the current field in the coastal waters of Zhejiang-Fujian to diminish, but the downcoast transport of CDW for at least 4 more days in the northern region of Zhejiang near the Changjiang River Estuary because of the buoyant coastal current (Zhang et al., 2018).

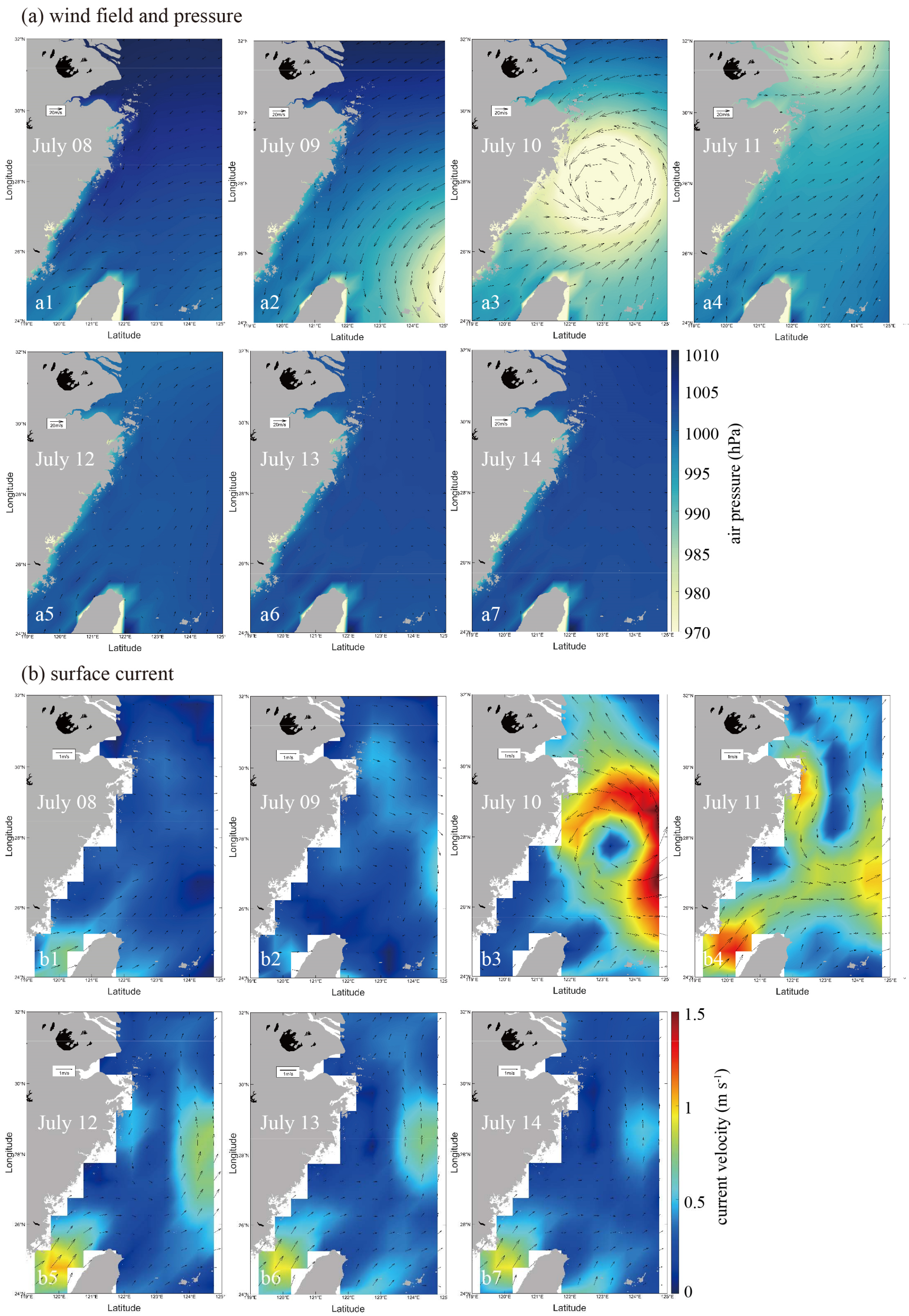

Figure 7. (a) Wind field and air pressure of ECS from July 8 to 14, 2015. The arrows represent the direction and velocity of wind, and the colors represent values of air pressure. The data was

obtained from ECMWF. (b) Surface current (0 m) of ECS from July 8 to 14, 2015. The arrows represent the direction and velocity of surface current, and the color also indicate the values of velocity. The data was obtained from CMEMS.

5.3 Residence time of typhoon-induced CDW in the study area

The downcoast transport of CDW triggered by Typhoon Chan-Hom brought a large volume of fresh water to the coast of Zhejiang and Fujian, and these CDW remained in the surface layer and distributed in a limited area for several days after the typhoon's transit.

Previous studies showed the strong presence of summer upwelling off the coast of Zhejiang Province north of 28.5°N (Li et al., 2022). The intrusion of low-temperature, high-salinity water was also observed at the bottom layer of transect IV's offshore end during the NCS (Figure 2a, b). Li et al. (2022) showed that the Ekman transport along the coast of Zhejiang and Fujian triggered by the wind field of Chan-Hom shifted with the movement of the typhoon, resulting in a transition of upwelling-downwelling-upwelling along the coast of Zhejiang and Fujian: as the typhoon first approached July 10, strong downwelling was mainly occurred along the coast of Zhejiang and Fujian. Upwelling appeared along the coast of Zhejiang July 11 and propagated downcoast in the form of coastal shelf waves. By July 14-15 (post-typhoon survey of this study), upwelling extended to the entire region (south of 28°N along the coast of Zhejiang and Fujian). These cool, saline seawater intrusion from the upwelling (Figure 2a) formed a strong pycnocline (Figure 2c) that inhibited the turbulent mixing and potentially hindered the downward transmission of CDW on the surface.

The post-typhoon current field in the study area gradually returned to typical summer ZFCC pattern, which helped spreading the CDW northward (Figure 6a). However, the buoyant coastal current north of the study area was directed downcoast and self-sustained until new external force occurred after Typhoon Chan-Hom (Chapman & Lentz, 1994; Zhang et al., 2018), and the cyclonic eddy occurred in the east of study area (Li et al., 2022, also seen in Figure 7, b3-b7) also led to a downcoast pumping of coastal water. These two forces greatly slowed down the upcoast retreat of CDW.

Assuming the diffusion is negligible (the vertical diffusive velocity was 4 – 5 orders of magnitude lower than the horizontal flow velocity according to Zhu et al., 2022), the residence time (t) of the low salinity water from CDW in the study area can be calculated:

$$Q_f = \sum_{i=1}^{M-1} \sum_{k=1}^{N} \frac{S_0 - S_{i,k}}{S_0} \times v_{i,k} \times h_{i,k} \times \Delta d_i \qquad (7)$$

$$t = \frac{V_f}{Q_f} \qquad (8)$$

Where Q_f is the freshwater discharge of northern boundary of study area (Transect IV), v is the velocity of background current after typhoon. As can be seen in Figure 6, the cross-shore water discharge in the study area after typhoon was nearly one orders of magnitude lower than the alongshore water discharge, so v was directly selected as the alongshore velocity. The calculated result shows that the low salinity water brought by the transit of Typhoon Chan-Hom can stay in the study area for about 13 days. It is worth noting that the water salinity in the study area would gradually decrease as freshwater was continuously transported northward, as well as freshwater discharge, thus it will inevitably lead to a shorter calculation of residence time because of taking the freshwater discharge of 14 July as the background discharge in this study. In addition, the upcoast transport of freshwater in the southern boundary (Transect I) to the study area also leads to an underestimation of the residence time, but it is certain that the removing of these abnormal freshwater in the study area requires at least 13 days. Our observations show that large volumes of low salinity water are no longer present in the study area 21 days after the typhoon's passage, and the contribution of CDW is reduced to 2-3% at that time (Figures 2 and 5). Therefore, the dispersion of CDW in the study area was limited after the typhoon's passage, and maintained in the surface layer of water column in the coastal region of Zhejiang and Fujian for 13-21 days. This long presence of the CDW in turn is believed to render ecological effects to the area.

5.4 Ecological impact of typhoon-induced CDW

5.4.1 Enhanced primary productivity indicated by Chlorophyll-a after Typhoon Chan-Hom

Increases of Chlorophyll-a in the surface water (Figure 3, a1) indicate that the nutrients in the typhoon-induced CDW must have significant impact on the ecological environment of the Zhejiang-Fujian coastal area and even the entire inner shelf of the ECS. In general, strong mixing by a passing typhoon creates a turbid water column where poor light transmission is not suitable for phytoplankton growth, although this process could pump the nutrients from near bottom or pore water to the surface water (Chen et al., 2017). In this study, however, low turbid CDW (Figure S2) dominated the post-typhoon surface waters (<10 m) in the study area, where a rapid phytoplankton bloom (Figure 3, a1) became possible. In contrast, the Chlorophyll-a concentration near the bottom of the water column were extremely low (<0.5 mg m^{-3}), primarily due to the high turbidity from resuspended sediments (Figure S2). Meamwhile, the strong stratification in the PTS indicates lillte contribution of verticle pumping to the additional nutients that led to a phytoplankton blooming in the study area after typhoon.

POC concentration (Figure 3b) in the surface water was also significantly higher, which may indicate higher primary productivity and organic carbon production in the typhoon-induced CDW. In addition, most of the $\delta^{13}C_{POC}$ in the areas with high POC concentration were <-20‰ (Figure 3c), suggesting a dominated marine source organic carbon produced by the in situ primary productivity. Chlorophyll-a and other primary productivity indicators in the water column returned to the pre-typhoon level 3 weeks after Chan-Hom's passing, evidenced by the mean value and distribution pattern obtained during the NCS (August 2015) that showed a typical summer pattern of inner shelf of ECS (Li et al., 2013).

5.4.2 Identification of suspended POM sources: contribution by primary productivity or terrestrial discharge

The sources of suspended POC in marine environment include exogenous and autogenous, of which the exogenous POC mainly derived from terrestrial plants and autogenous POC mainly produced by plankton in marine ecosystems (Li et al., 2012a; Gao et al., 2014). Obviously, resuspension of bed sediments is also an important source of suspended POC in the water column, but these POC may include organic matter of both marine and terrestrial origin, and thus their chemical characteristics depend largely on the characteristics of the sediments (Gao et al., 2014). The linear relationships between POC and SPM showed that POC was significantly and positively correlated with SPM in the bottom waters with R^2 of 0.46 (n = 63) and 0.64 (n = 58) for PTS and NCS, respectively, whereas the surface water samples showed only a weak correlation in the NCS (R^2 = 0.26, n = 42) and no correlation in the PTS (Figure 8 a-c). This suggests that the POC in the bottom waters of the study area is mainly controlled by SPM, while the surface waters show significant differences between the two surveys: the surface waters was also influenced by SPM in the NCS but completely unaffected by SPM in the PTS, which may be more influenced by the CDW-induced increase in primary productivity.

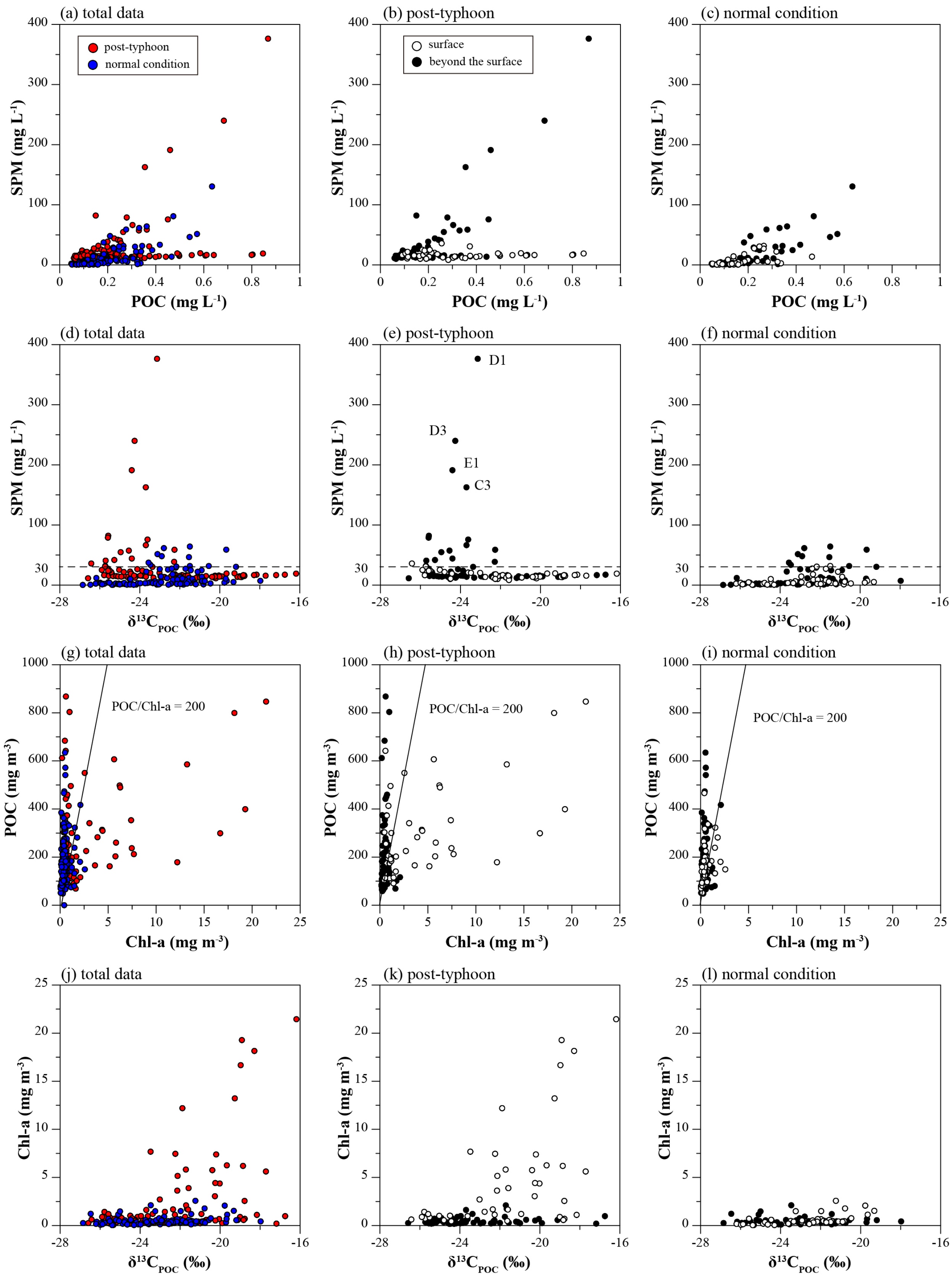
(a) total data
post-typhoon
normal condition
SPM (mg L-1)
POC (mg L-1)
(b) post-typhoon
surface
beyond the surface
(c) normal condition
(d) total data
δ13CPOC (‰)
(e) post-typhoon
D1
D3
E1
C3
(f) normal condition
(g) total data
POC/Chl-a = 200
POC (mg m-3)
Chl-a (mg m-3)
(h) post-typhoon
(i) normal condition
(j) total data
(k) post-typhoon
(l) normal condition

Figure 8. Bi-plots showing the relationships of (a-c) SPM vs. POC, (d-f) SPM vs. $\delta^{13}C_{POC}$, (g-i) POC vs. Chl-a, and (j-l) Chl-a vs. $\delta^{13}C_{POC}$ for the total samples (left panel), post-typhoon (middle panel), and normal condition (right panel). The red dots represent samples collected in the post-typhoon state and the blue dots represent samples collected in the post-typhoon state. The hollow circles represent surface samples collected in depth <10 m and solid circles represent samples collected in depth >10 m.

$\delta^{13}C_{POC}$ is one of the most important indicators for the identification of organic carbon sources due to the different degrees of isotopic fractionation caused by the uptake and utilization of CO_2 by terrestrial plants and marine phytoplankton, which eventually leads to differences in the generated $\delta^{13}C$ values (Li et al., 2012a). In this study, the $\delta^{13}C_{POC}$ showed much greater range of variation with low SPM (< 30 mg L-1), indicating a complex source of POC in low SPM water (Figure 8 d-f). In contrast, the $\delta^{13}C_{POC}$ is fairly constant with high SPM (> 30 mg L-1), but there were obvious difference in values between PTS and NCS: the $\delta^{13}C_{POC}$ ranged from -26 to -22‰ and was consisted in -24 with higher SPM (SPM > 100 mg L-1) in the PTS, which was lower than that in the NCS (ranged from -24 to -20‰). In addition, high SPM mainly occurred in the bottom water and was significant higher in the PTS than in the NCS. Previous studies showed that, the $\delta^{13}C$ of sediments in the inner shelf of ECS ranged from -23.1 to -20.9‰ (Li et al., 2012a), thus, the suspended POC in the bottom water collected during NCS may be derived from the resuspension of sediments (Figure 8f). However, the $\delta^{13}C$ in the POC collected from bottom water during PTS was significantly lower than that of the sediment, suggesting that these POC may be affected by sources or processes other than sediment resuspension. Unfortunately, the data in this study are not sufficient to reveal this specific process.

The molar carbon to nitrogen ratio (C/N) is another indicator to identify the source of POM (Liu et al., 2018). The linear relationships between POC and PN (Figure S3), which were POC = 5.92 PN - 4.06 (R^2=0.973, n=106) and POC = 6.04PN + 0.11 (R^2=0.866, n=99) in the PTS and NCS, respectively, suggest that the nitrogen is strongly accosiated with organic carbon in the study area. The slopes of linear regression of POC against PN indicated a molar C/N ratio of 5.92 and 6.04 in the PTS and NCS, respectively. They were both lower but closed to the Refield Ratio (6.63), and similar to the average molar ratios of 5.6 for marine POM (Copin-Montegut and Copin-Montegut, 1983) and the results of summer Southern ECS reported by Liu et al. (2018). The narrow range of low C/N in this study confirm the lack of terrestrial signals transported mainly by the Changjiang River, especially in the PTS, although there was large volume of CDW transported to the study area. Thus, the POM in study area was mainly dominated by marine source both in the NCS and PTS. In addition, low C/N ratios further restrict the assumption of degradation of nitrogen-rich organic matter, a process that normally increases the C/N ratio to more than that of the Redfield ratio (Liu et al. 2018). Since the C/N in the post-typhoon condition was close to that in the normal condition as mentioned above, this parameter cannot used to identify the impact of the phytoplankton bloom caused by Typhoon Chan-Hom. Therefore, we analyzed the relationships of POC vs. Chl-a and Chl-a vs. $\delta^{13}C_{POC}$ to further quantify the contribution of primary productivity to the POC in both PTS and NCS.

The POC/Chl-a ratio has also been used to discriminate the sources of POM in the coastal region and shelf seas (Cifuents et al., 1988; Liu et al., 2018). In the previous studies (Cifuentes et al., 1988; Liu et al., 2018), a POC/Chl-a ratio of 200 g g^{-1} was used to identify the predominance of newly produced phytoplankton (or autotrophic-dominated) in POM (< 200 g g^{-1}) and detrital or degraded organic matter (or heterotrophic/mixture-dominated) (>200 g g^{-1}). The POC/Chl-a ranged from 14.64 to 3060.23 g g^{-1} (averaged 367.71 g g^{-1}) in the PTS and 54.43 to 3209.79 g g^{-1} (averaged 547.69 g g^{-1}) in the NCS. The POC/Chl-a of most POM were higher than 200 g g^{-1}, especially the POM collected in the whole water column during NCS, and only part of POM collected in the surface water during PTS, suggesting that the POM in the study area was dominated by the detrital or degraded organic matter, which may be derived from resuspension sdiments as the results discussed by $\delta^{13}C_{POC}$ vs. SPM, whereas the primary productivity mainly contributed in the surface water during PTS. In the normal summer condition, the primary productivity is lower due to the nutrient limiting, thus the POM concentration in water colume was relative low and mainly contributed by sediment resuspension. However, as discussed above, the passing of Typhoon Chan-Hom induced downcoast transport of CDW, which brought large amout of nutrients and led to phytoplankton in the surface layer of the study area, changing the ecological pattern of the Zhejiang-Fujian coastal area and even the entire inner shelf of the ECS.

5.4.3 Special significance of ecological effects induced by Typhoon Chan-Hom

Not only the present study, but also a large number of previous studies have shown that typhoons can trigger significant ecological effects in the affected local waters, mainly in the form of significant increase in chlorophyll-a and POC caused by phytoplankton blooms (Hung et al., 2010; Hung and Gong 2011; Wang et al., 2017). However, there are significant differences in the triggering mechanisms of the ecological effects induced by typhoons due to regional differences. Estuarine regions are more susceptible to enhanced riverine input of nutrients and water column vertical mixing induced by typhoon (Wang et al., 2018), coastal regions are more affected by typhoon-induced upwelling (Hung and Gong 2011; Li et al., 2022), and in open oceans are controlled by vertical mixing of water column (Lin et al., 2003; Pana et al., 2017). Previous studies have shown that typhoon-induced flooding of the Yangtze River triggers phytoplankton blooming but limits in the Changjiang River estuary and surrounding waters in summer due to the northward ZFCC (Wang et al., 2017). In contrast, Changjiang River materials (including dissolved and particulate matters) are mainly transported to the of Zhejiang-Fujian coast by the southward ZFCC in winter (Jan et al., 2002; Wu et al., 2013). Therefore, most studies attribute the increase in primary productivity along the Zhejiang-Fujian coast after typhoon transit to upward nutrients supplying by typhoon-induced vertical mixing and upwelling (Li et al., 2013; Li et al., 2022). However, this study confirms that the downcoast transport of CDW caused by typhoon processes also carries a large amount of nutrients to the Zhejiang-Fujian coast in summer and led to a significant enhanced primary productivity. It is worth noting that not all typhoons that passing through the ECS result in downcoast transport of CDW. For instance, the 2008 Typhoon Morakot did not produce a downcoast transport of large volume of CDW (Li et al., 2013). The difference is determined by the typhoon's path: Typhoon Chan-Hom's route was north of the study area and had a relatively large impact on the Changjiang River Estuary (including runoff and currents), whereas Typhoon Morakot passed south of the study area, away from the Changjiang River Estuary and the CDW. The cyclonic structure of a typhoon can lead to dynamic asymmetry on the two sides of its path. In general, typhoon-induced coastal storm surge is higher on the right side of path, causing stronger surface currents (Wu et al., 2021; also seen in Figure 7, b3). Thus, typhoon-induced changes of hydrodynamic conditions and material transport processes in a certain area cannot be generalized for typhoon with different paths (Li et al., 2018).

This study demonstrates that typhoons passing the Changjiang River Estuary can trigger downcoast transport of CDW as far as 27°N off the coast of Zhejiang and Fujian. More importantly, the CDW on the inner shelf of the ECS stay on for several more days after typhoon's passage. Inevitably, the Changjiang River source materials carried by the CDW will have a significant impact on the physical, chemical and biological processes in the marine environment of the ECS. Previous studies have focused mainly on the impact of the Changjiang River source material brought by the downcoast ZFCC in winter on the inner shelf of the ECS (Deng et al., 2017; Liu et al., 2018; Liu et al., 2021 and reference therein), often ignoring the role of typhoons in summer. Statistics show that, an average of 2 typhoons affected the Changjiang River Estuary each year since 1961, and their intensity (mainly reflected in the magnitude of wind speed) have shown an upward trend, especially since the 1990s (Figure S4). Further studies on the mechanism, flux, duration and recovery time of CDW downcoast transport triggered by different typhoons are of importance for quantifying CDW's impact on the inner shelf sedimentary and environmental processes of the ECS.

6 Conclusions

This study quantitively details typhoon-induced downcoast transport of freshwater from Changjiang Diluted Water (CDW), which formed a shoreline-parallel low salinity (as low as 25.02) water strip, up to 70 km wide and 20 m thick, along the Zhejiang-Fujian coastal area with an estimated freshwater volume of 3.7×10^{10} m^3. A three-endmembers mixing model shows that the contribution of the CDW to the study area's surface waters (<10 m) immediately after the typhoon was as high as 32% (maximum 40%), much greater than the contribution under normal summer conditions of 3% (maximum 8%). The steady northerly wind at the front of the typhoon's wind field was responsible for a persistent downcoast water discharge (~5×10^5 m^3 s^{-1}) before typhoon's passage, and the downcoast water discharge was increased 2-3 folds (~15×10^5 m^3 s^{-1}) during typhoon's passage. It took only 3-4 days for the typhoon's effect on the current field in the coastal waters of Zhejiang-Fujian to diminish, and the upcoast water transport after typhoon was on average only 16% of the downcoast water transport during typhoon. These CDW remained in the study area for 13-21 days after the typhoon's passage, which was limited by the upwelling, buoyant coastal current, and cyclonic eddy. The cool, saline seawater intrusion from upwelling during typhoon formed a strong pycnoline that potentially hindered the downward diffusion of CDW on the surface. The presence of downcoast directed buoyant coastal current north of the study area and the cyclonic eddy pumping in the ECS greatly slowed down the upcoast retreat of CDW. Additional nutrients in the low turbid CDW also elevated the Chlorophyll-a concentration in the upper water column (mean 3.74 mg m^{-3}) and produced large amount of particulate organic carbon (mean 0.25 mg L^{-1}). As the intensity of typhoons that influenced the Changjiang River Estuary increased, further studies should focus more on CDW downcoast transport triggered by typhoons, which may have significant impact on the inner shelf sedimentary and environmental processes of the ECS.

Acknowledgments

We thank all the investigators for their help in collecting data during the surveys. Thanks to Fukang Qi for the help in data processing. This work was supported by the National Natural Science Foundation of China (41976050), and the Scientific Research Foundation of the Third Institute of Oceanography, MNR (TIO2019028, TIO2015014).

Open Research

The typhoon track data are available in Weather China (http://typhoon.weather.com.cn/). The 10 m wind field data was obtained from the reanalysis product of ERA5-Interim (http://apps.ecmwf.int/datasets/data/mediate_full_daily/) of the European Centre for Medium-Range Weather Forecasts (ECMWF). The sea surface current data was obtained from the French Copernicus Marine Environment Monitoring Service (CMEMS) (http://marine.copernicus.eu/). Observation data inquiries can be directed to the corresponding author.

References

Andersson, A.（2011). A systematic examination of a random sampling strategy for source apportionment calculations. *Science of the Total Environment, 412–413* (0), 232–238.

Beardsley, R. C., Limeburner, R., Yu, H., & Cannon, G. A. (1985). Discharge of the Changjiang (Yangtze river) into the East China sea. *Continental Shelf Research*, *4*(1-2), 57-76.

Chai, C., Yu, Z., Song, X., & Cao, X. (2006). The Status and Characteristics of Eutrophication in the Yangtze River (Changjiang) Estuary and the Adjacent East China Sea, China. *Hydrobiologia*, *563*(1), 313-328. doi: 10.1007/s10750-006-0021-7

Chang, P. -H., & Isobe, A. (2003). A numerical study on the Changjiang diluted water in the Yellow and East China Seas. *Journal of Geophysical Research*, *108*(C9), 3299. doi: 10.1029/2002jc001749

Chapman, D. C., & Lentz, S. J. (1994). Trapping of a coastal density front by the bottom boundary layer. *Journal of Physical Oceanography*, 24(7), 1464–1479.

Chen, C., Liu, H., & Beardsley, R.C. (2003). An unstructured grid, finite-volume, three-dimensional, primitive equations ocean model: Application to coastal ocean and estuaries.

Journal of Atmospheric and Oceanic Technology, 20, 159–186. doi: 10.1175/1520-0426(2003)020<0159:AUGFVT>2.0.CO;2.

Chen, C., Beardsley, R.C., & Cowles, G. (2006). An unstructured-grid, finite-volume coastal ocean model (FVCOM) system. *Oceanography, 19*, 78–89. doi: 10.5670/ oceanog.2006.92.

Chen, D., He, L., Liu, F., & Yin, K. (2017). Effects of typhoon events on chlorophyll and carbon fixation in different regions of the East China Sea. *Estuarine, Coastal and Shelf Science*, *194*, 229-239. doi: 10.1016/j.ecss.2017.06.026.

Chu, D., Zhang, J., Wu, Y., Jiao, X., & Qian, S. (2019). Sensitivities of modelling storm surge to bottom friction, wind drag coefficient, and meteorological product in the East China Sea. *Estuarine, Coastal and Shelf Science*, *231*, 106460. doi: 10.1016/j. ecss.2019.106460.

Cifuentes, L.A., Sharp, J.H., & Fogel, M.L. (1988). Stable carbon and nitrogen isotopes biogeochemistry in the Delaware estuary. *Limology and Oceanography, 33*, 1102-1115.

Cong, S., Wu, X., Ge, J., Bi, N., Li, Y., Lu, J., & Wang, H. (2021). Impact of Typhoon Chan-hom on sediment dynamics and morphological changes on the East China Sea inner shelf. *Marine Geology*, *440*, 106578. doi: 10.1016/j.margeo.2021.106578

Copin-Montegut, C., & Copin-Montegut, G. (1983). Stoichiometry of carbon, nitrogen, and phosphorus in marine particulate matter. *Deep-Sea Research: Part A, 30*, 31-46.

Deng, B., Wu, H., Yang, S., & Zhang, J. (2017). Longshore suspended sediment transport and its implications for submarine erosion off the Yangtze River Estuary. *Estuarine, Coastal and Shelf Science*, *190*, 1-10. doi: 10.1016/j.ecss.2017.03.015

Gao, L., D. Li, and J. Ishizaka (2014). Stable isotope ratios of carbon and nitrogen in suspended organic matter: Seasonal and spatial dynamics along the Changjiang (Yangtze River) transport pathway. *Journal of Geophysical Research: Biogeosciences, 119*, 1717–1737.

doi:10.1002/2013JG002487.

He, X., Bai, Y., Chen, C.-T. A., Hsin, Y.-C., Wu, C.-R., Zhai, W., Liu, Z., & Gong, F. (2014). Satellite views of the episodic terrestrial material transport to the southern Okinawa Trough driven by typhoon. *Journal of Geophysical Research: Oceans, 119*(7), 4490-4504.Hou, W., Ba, M., Bai, J., & Yu, J. (2021). Numerical Study on the Expansion and Variation of Changjiang Diluted Water in Summer and Autumn. *Journal of Marine Science and Engineering*, *9*(3). doi: 10.3390/jmse9030317

Hung C.-C. & Gong G.-C. (2011). Biogeochemical responses in the southern East China Sea after typhoon. *Oceanography, 24(4)*, 42-51.

Hung C.-C., Gong G.-C., Chou W.C., Chuang, C.C., Lee M.A., Chang, Y., Chen, H.-Y, Huang, S.-J., Yang, Y., Yang, W.-R, Chung W.-C., Li, S.-L., & Law, E. (2010). The effect of typhoon on particulate organic carbon flux in the southern East China Sea. *Biogeosciences, 7*, 3007-3018.

Jan, S., Wang, J., Chern, C., & Chao, S. (2002). Seasonal variation of the circulation in the Taiwan Strait. *Journal of Marine Systems*, *35*, 249-268.

Lee, J. H., Moon, I.-J., Moon, J.-H., Kim, S.-H., Jeong, Y. Y., & Koo, J.-H. (2017). Impact of typhoons on the Changjiang plume extension in the Yellow and East China Seas. *Journal of Geophysical Research: Oceans*, *122*(6), 4962-4973. doi: 10.1002/2017jc012754

Li, D., Zhang, J., Huang, D., Wu, Y., & Liang, J. (2002). Oxygen depletion off the Changjiang (Yangtze River) Estuary. *Science in China Series D: Earth Sciences*, *45*(12), 1137-1146.

Li, H.-M., Tang, H.-J., Shi, X.-Y., Zhang, C.-S., & Wang, X.-L., (2014). Increased nutrient loads from the Changjiang (Yangtze) River have led to increased Harmful Algal Blooms. *Harmful Algae*, *39*, 92-101. doi: 10.1016/j.hal.2014.07.002.

Li, X., Bianchi, T.S., Allison, M.A., Chapman, P., Mitra, S., Zhang, Z., Yang, G.P., & Yu, Z.G. (2012a). Composition, abundance and age of total organic carbon in surface sediments from the inner shelf of the East China Sea. *Marine Chemistry, 145-147*, 37-52.

Li, Y., Xu, X., & Zheng, B. (2018). Satellite views of cross-strait sediment transport in the Taiwan Strait driven by Typhoon Morakot (2009). *Continental Shelf Research*, *166*, 54-64. doi: 10.1016/j.csr.2018.07.004.

Li, Y., Wang, A., Qiao, L., Fang, J., & Chen, J. (2012b). The impact of typhoon Morakot on the modern sedimentary environment of the mud deposition center off the Zhejiang–Fujian coast. China, *Continental Shelf Research*, *37*, 92-100. doi: 10.1016/j.csr.2012.02.020.

Li, Y., Yang, D., Xu, L., Gao, G., He, Z., Cui, X., et al. (2022). Three types of typhoon-induced upwellings enhance coastal algal blooms: A case study. Journal of Geophysical Research: Oceans, 127, e2022JC018448.

Li, Y., Ye, X., Wang, A., Li, H., Chen, J., & Qiao, L. (2013). Impact of Typhoon Morakot on chlorophyll a distribution on the inner shelf of the East China Sea. *Marine Ecology Progress Series*, *483*, 19-29. doi: 10.3354/meps10223.

Lie, H.-J., Cho, C.-H., Lee, J.-H., & Lee, S. (2003). Structure and eastward extension of the Changjiang River plume in the East China Sea. *Journal of Geophysical Research*, *108*(C3), 3077. doi: 10.1029/2001jc001194.

Lin, I., Liu, W. T., Wu, C.-C., Wong, G. T. F., Hu, C., Chen, Z., Liang, W.-D., Yang, Y., & Liu, K.-K. (2003). New evidence for enhanced ocean primary production triggered by tropical cyclone. *Geophysical Research Letters*, *30*(13), 1718. doi: 10.1029/2003GL017141.

Liu, J. T., Lee, J., Yang, R. J., Du, X., Li, A., Lin, Y.-S., Su, C.-C., & Tao, S. (2021). Coupling between physical processes and biogeochemistry of suspended particles over the inner shelf mud in the East China Sea. *Marine Geology*, *442*. doi: 10.1016/j.margeo.2021.106657.

Liu, J. T., Hsu, R. T., Yang, R. J., Wang, Y. P., Wu, H., Du, X., Li, A., Chien, S. C., Lee, J., Yang, S., Zhu, J., Su, C.-C., Chang, Y., & Huh, C.-A. (2018). A comprehensive sediment dynamics study of a major mud belt system on the inner shelf along an energetic coast. *Scientific reports*, *8*(1), 4229. doi: 10.1038/s41598-018-22696-w.

Liu, Q., Kandasamy, S., Lin, B., Wang, H., & Chen, C.-T. A. (2018). Biogeochemical characteristics of suspended particulate matter in deep chlorophyll maximum layers in the southern East China Sea. *Biogeosciences, 15*, 2091-2109, https://doi.org/10.5194/bg-15-2091-2018.

Liu, Q., Kandasamy, S., Wang, H., Wang, L., Lin, B., Gao, A., & Chen, C.-T. A. (2019). Impact of hydrological conditions on the biogeochemical dynamics of suspended particulate organic matter in the upper mixed layer of the southern East China Sea. *Journal of Geophysical Research: Oceans, 124*, 6120- 6140. https://doi.org/10.1029/2019JC015193.

Pana, G., Chai, F., Tang, D. L., & Wang, D. X. (2017). Marine phytoplankton biomass responses to typhoon events in the South China Sea based on physical-biogeochemical model. *Ecological Modelling*, *356*, 38-47. doi: 10.1016/j.ecolmodel.2017.04.013.

Saha, S., et al. (2011). NCEP Climate Forecast System Version 2 (CFSv2) Selected Hourly Time-Series Products, https://doi.org/10.5065/D6N877VB, Research Data Archive at the National Center for Atmospheric Research, Computational and Information Systems Laboratory, Boulder, Colo. (Updated monthly.) Accessed 1 Oct 2022.

Shang, F., Qiao, F., & Xia, C. (2009). A numerical study of summertime expansion pattern of Changjiang (Yangtze) River diluted water. *Acta Oceanologica Sinica*, *28*(3), 11-16.

Su, J. L. (2005). The Oceanography in the Chinese Margin Sea (in Chinese). Ocean Press, Beijing.

Tong, Y., Zhao, Y., Zhen, G., Chi, J., Liu, X., Lu, Y., Wang, X., Yao, R., Chen, J., & Zhang, W. (2015). Nutrient Loads Flowing into Coastal Waters from the Main Rivers of China (2006-2012), *Scientific reports*, *5*, 16678. doi: 10.1038/srep16678

Wang, B., Chen, J., Jin, H., Li, H., Huang, D., & Cai, W. J. (2017). Diatom bloom-derived bottom water hypoxia off the Changjiang estuary, with and without typhoon influence. *Limnology and Oceanography*, *62*(4), 1552-1569. doi: 10.1002/lno.10517

Wu, H., Deng, B., Yuan, R., Hu, J., Gu, J., Shen, F., Zhu, J., & Zhang, J. (2013). Detiding Measurement on Transport of the Changjiang-Derived Buoyant Coastal Current. *Journal of Physical Oceanography*, *43*(11), 2388-2399. doi: 10.1175/jpo-d-12-0158.1

Wu, R., Wu, S., Chen, T., Yang, Q., Han, B., & Zhang, H. (2021). Effects of Wave–Current Interaction on the Eastern China Coastal Waters during Super Typhoon Lekima (2019). *Journal of Physical Oceanography*, *51*(5), 1611-1636. doi: 10.1175/jpo-d-20-0224.1

Wu, T., & Wu, H. (2018). Tidal Mixing Sustains a Bottom-Trapped River Plume and Buoyant Coastal Current on an Energetic Continental Shelf. *Journal of Geophysical Research: Oceans*, *123*(11), 8026-8051. doi: 10.1029/2018jc014105

Wu, Y., Zhang, J., Li, D. J., Wei, H., & Lu, R. X. (2003). Isotope variability of particulate organic matter at the PN section in the East China Sea. *Biogeochemistry, 65*, 31–49.

Yanagi, T., Takahashi, S., Hoshika, A., & Tanimoto, T. (1996). Seasonal variation in the transport of suspended matter in the East China Sea. *Journal of Oceanography*, 52, 539-552.

Yang, S., & Yin, P. (2018). Sediment source-to-sink processes ofsmall mountainous rivers under the impacts of natural environmental changes and human activities (in Chinese with English abstract). *Mar. Geol. Quat. Geol.*, *38*(1), 1–10. doi: 10.16562/j.cnki.0256-1492.2018.01.001

Yang, S. L., Milliman, J. D., Xu, K. H., Deng, B., Zhang, X. Y., & Luo, X. X. (2014). Downstream sedimentary and geomorphic impacts of the Three Gorges Dam on the Yangtze River. *Earth-Science Reviews*, *138*, 469-486. doi: 10.1016/j.earscirev.2014.07.006

Zhang, Z., Wu, H., Yin, X., & Qiao, F. (2018). Dynamical Response of Changjiang River Plume to a Severe Typhoon With the Surface Wave-Induced Mixing. *Journal of Geophysical Research: Oceans*, *123*(12), 9369-9388. doi: 10.1029/2018jc014266

Zhou, M. J., Shen, Z. L., & Yu, R. C. (2008). Responses of a coastal phytoplankton community to increased nutrient input from the Changjiang (Yangtze) River. *Continental Shelf Research*, *28*(12), 1483-1489. doi: 10.1016/j.csr.2007.02.009

Zhu, B., Yang, W., Jiang, C., Wang, T., & Wei, H. (2022). Observations of turbulent mixing and vertical diffusive salt flux in the Changjiang Diluted Water. *Journal of Oceanology and Limnology*, 1-12.

Zhu, J., Chen, C., Ding, P., Li, C., & Lin, H. (2004). Does the Taiwan warm current exist in winter? *Geophysical research letters*, *31*(12): 1-4.

Journal of Geophysical Research: Oceans

Supporting Information for

Downcoast Redistribution of Changjiang Diluted Water due to Typhoon Chan-Hom (2015)

Yunpeng Lin[1], Yunhai Li[2, 3*], Shuai Cong[4], Meng Liu[1], Liang Wang[3], Binxin Zheng[3], Jingping Xu[1, 2*]

[1]Department of Ocean Science & Engineering, Southern University of Science and Technology, China.

[2] Laboratory for Marine Geology, Qingdao National Laboratory for Marine Science and Technology, China.

[3]Third Institute of Oceanography, Ministry of Natural Resources, China.

[4]College of Marine Geosciences, Key Laboratory of Submarine Geosciences and Prospecting Techniques, Ocean University of China, China.

Corresponding author: Yunhai Li (liyunhai@tio.org.cn), Jingping Xu (xujp@sustech.edu.cn)

Contents of this file

Figures S1 to S4

Tables S1 and S2

Introduction

Two additional figures were provided here as supporting information for our manuscript "Downcoast Redistribution of Changjiang Diluted Water due to Typhoon Chan-Hom (2015)''.

Figure S1 plots the precipitation during Typhoon Chan-Hom (9-12 July) in the East China Sea and eastern China. The precipitation was mainly occurred in the East China, and there was little precipitation in the drainage basin of Oujiang River.

Figure S2 plots the water turbidity in the study area immediately after the passing of Typhoon Chan-Hom and 3 weeks later. In the post-typhoon condition, the turbidity ranged from 0.26 to

855.74 FTU (averaged 26.79 FTU) in the water column, and the high turbidity was mainly occurred in the bottom layer. However, in the normal condition, the turbidity ranged from 0.1 to 355.92 FTU (averaged 16.93 FTU), which were significantly lower than that in the post-typhoon condition, and the high value also occurred in the bottom layer.

Figure S3 is the bi-plot showing the relationships of POC vs. PN in the post-typhoon and normal condition states.

Figure S4 plots the number and wind speed of typhoons influenced Changjiang River Estuary (passed north of study area) during 1961-2022. The information was collected from http://www.wztf121.com/.

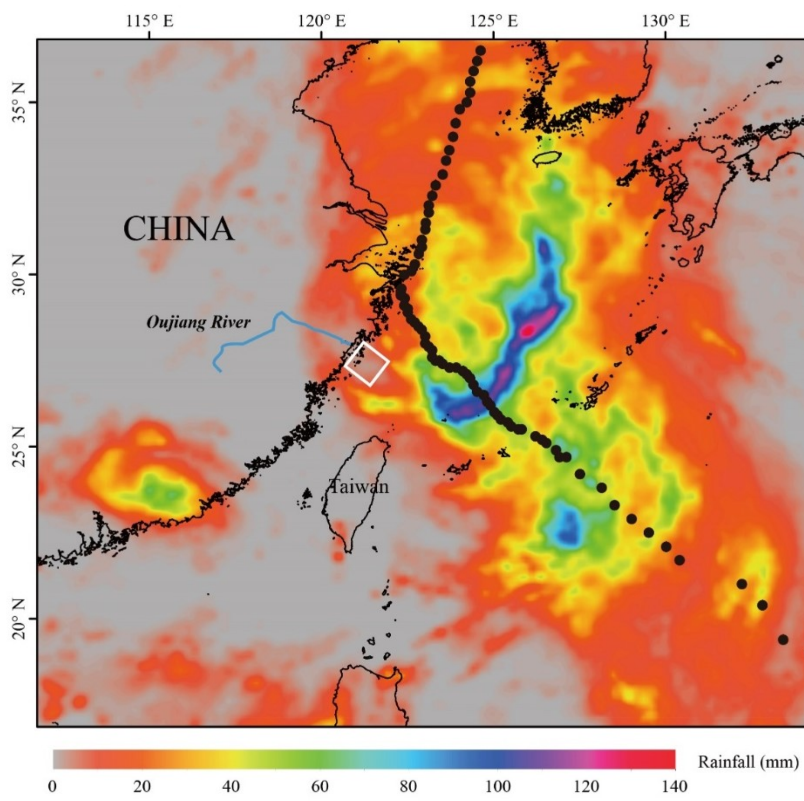

Figure S1. Distribution of total rainfall from July 9 to 12, 2015 under the influence of Typhoon Chan-Hom. The black dots indicate the track of Typhoon Chan-Hom. The different colors represent rainfall amount (mm). The highest rainfall occurred in the offshore area of East China Sea. The white box indicates study area located in the Zhejiang-Fujian costal area.

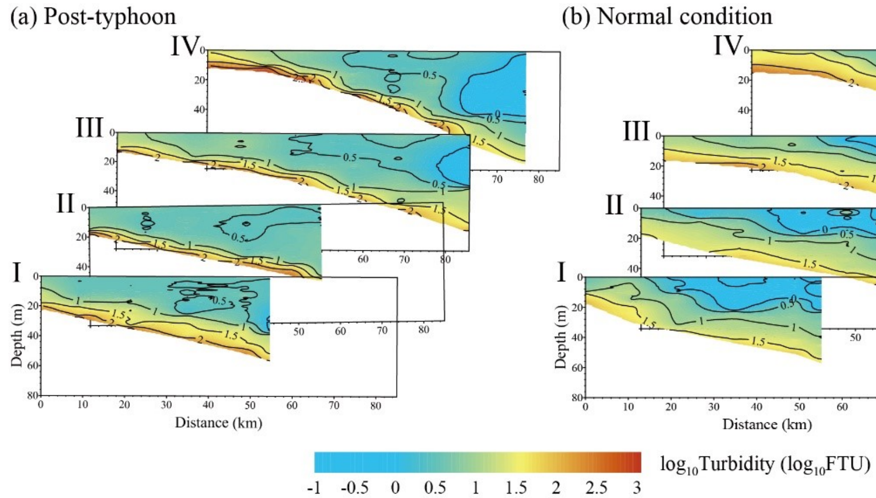

Figure S2. The measured turbidity ($\log_{10}$ value) along 4 cross-shelf transects immediately after the passing of Typhoon Chan-Hom (left panels) and 3 weeks later (right panels)

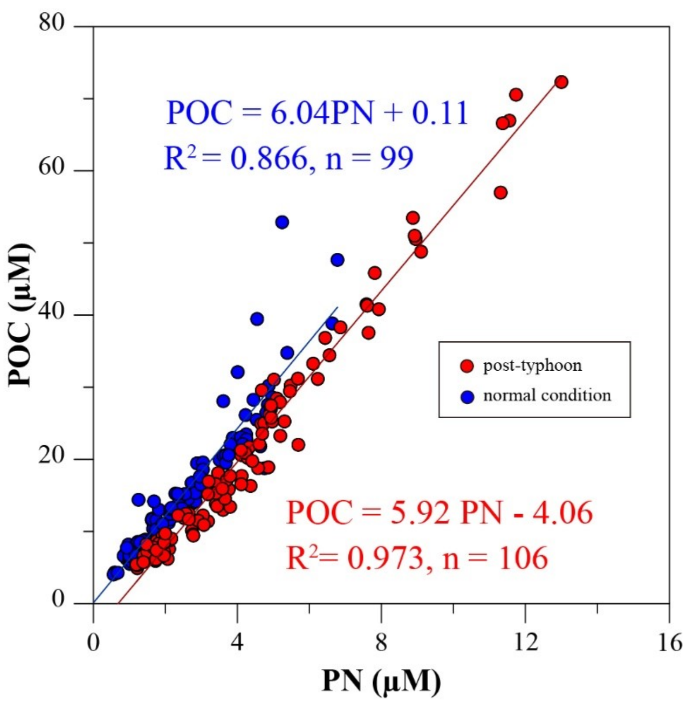

Figure S3. Bi-plot showing the relationships of POC vs. PN in the post-typhoon and normal condition states.

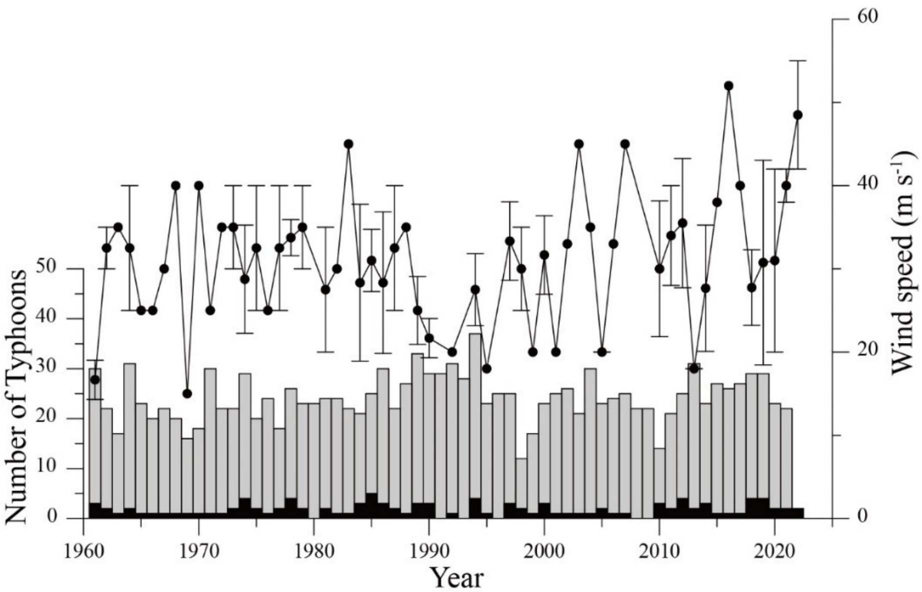

Figure S4. The number and wind speed of typhoons influenced Changjiang River Estuary (passed north of study area) during 1961-2022. The gray column is number of total typhoons that produced in the west Pacific Ocean and black number is the number of typhoons that influenced Changjiang River Estuary. The black point is the average wind speed with error bar of typhoons when they affected Changjiang River Estuary.

Table S1. The mean, minimum, and maximum contribution values of different endmembers and standard deviation of each sample in NCS calculated by three-endmember mixing model.

Sample	CDW				SSW				SBW			
	mean	min	max	std	mean	min	max	std	mean	min	max	std
E10-1	11%	8%	16%	0.01	45%	34%	62%	0.03	43%	27%	53%	0.03
E10-2	18%	14%	26%	0.01	41%	27%	57%	0.03	41%	25%	51%	0.03
E10-3	20%	15%	28%	0.01	39%	25%	56%	0.03	41%	25%	51%	0.03
E10-4	27%	20%	38%	0.02	39%	22%	58%	0.04	34%	16%	46%	0.03
E10-5	27%	20%	37%	0.02	45%	27%	66%	0.04	28%	9%	40%	0.03
E10-6	27%	20%	37%	0.02	56%	37%	77%	0.04	18%	0%	31%	0.04
A1-1	10%	8%	14%	0.01	46%	35%	63%	0.03	44%	27%	53%	0.03
A1-2	10%	8%	15%	0.01	46%	35%	63%	0.03	44%	27%	53%	0.03
A1-3	13%	9%	18%	0.01	44%	32%	60%	0.03	43%	27%	53%	0.03
A1-4	24%	18%	33%	0.02	31%	16%	47%	0.03	45%	30%	55%	0.02
A1-5	27%	20%	38%	0.02	29%	13%	46%	0.03	44%	28%	54%	0.03
A1-6	32%	24%	45%	0.02	41%	20%	62%	0.04	27%	7%	40%	0.03
A2-1	32%	24%	45%	0.02	42%	22%	64%	0.04	25%	5%	39%	0.03
A2-2	31%	23%	44%	0.02	38%	19%	58%	0.04	31%	12%	43%	0.03
A2-3	28%	21%	40%	0.02	27%	10%	44%	0.03	44%	29%	54%	0.03
A2-4	26%	20%	37%	0.02	29%	13%	45%	0.03	45%	29%	54%	0.02
A2-5	9%	6%	12%	0.01	46%	35%	63%	0.03	45%	29%	55%	0.03
A2-6	6%	4%	8%	0.00	53%	42%	73%	0.03	41%	22%	52%	0.03
A3-1	4%	3%	6%	0.00	55%	44%	75%	0.03	41%	22%	52%	0.03
A3-2	4%	3%	6%	0.00	55%	43%	74%	0.03	41%	22%	52%	0.03
A3-3	4%	3%	6%	0.00	55%	43%	74%	0.03	41%	22%	52%	0.03
A3-4	7%	5%	11%	0.01	49%	37%	66%	0.03	44%	27%	54%	0.03
A3-5	22%	16%	30%	0.01	32%	18%	48%	0.03	46%	31%	55%	0.02
A3-6	32%	24%	44%	0.02	46%	25%	68%	0.04	22%	1%	36%	0.03
A4-1	36%	27%	50%	0.02	47%	24%	68%	0.05	17%	0%	32%	0.04
A4-2	36%	27%	50%	0.02	41%	19%	63%	0.04	24%	3%	37%	0.03
A4-3	29%	22%	40%	0.02	29%	12%	46%	0.03	42%	27%	53%	0.03
A4-4	16%	12%	23%	0.01	38%	26%	53%	0.03	45%	31%	54%	0.02
A4-5	5%	4%	7%	0.00	47%	36%	64%	0.03	48%	32%	58%	0.03
A4-6	4%	3%	6%	0.00	45%	35%	61%	0.03	51%	35%	60%	0.03
A5-1	4%	3%	5%	0.00	44%	34%	59%	0.03	53%	38%	62%	0.03
A5-2	4%	3%	5%	0.00	46%	36%	62%	0.03	51%	35%	60%	0.03
A5-3	4%	3%	6%	0.00	54%	43%	74%	0.03	42%	23%	53%	0.03
A5-4	4%	3%	6%	0.00	59%	46%	80%	0.04	37%	17%	49%	0.03
A5-5	10%	8%	15%	0.01	46%	35%	63%	0.03	43%	27%	53%	0.03

A5-6	33%	25%	46%	0.02	39%	18%	59%	0.04	29%	9%	41%	0.03
E9-1	12%	9%	17%	0.01	44%	33%	61%	0.03	44%	28%	53%	0.03
E9-2	24%	18%	34%	0.02	36%	20%	53%	0.03	40%	23%	50%	0.03
E9-3	25%	19%	35%	0.02	42%	25%	61%	0.04	33%	15%	44%	0.03
E9-4	28%	21%	39%	0.02	47%	28%	69%	0.04	25%	5%	38%	0.03
E9-5	30%	22%	42%	0.02	62%	41%	76%	0.04	8%	0%	23%	0.04
E9-6	30%	23%	42%	0.02	64%	43%	77%	0.04	6%	0%	21%	0.03
B1-1	9%	7%	13%	0.01	45%	34%	61%	0.03	46%	30%	55%	0.03
B1-2	10%	7%	14%	0.01	45%	34%	61%	0.03	46%	30%	55%	0.03
B1-3	16%	12%	23%	0.01	37%	25%	52%	0.03	47%	32%	55%	0.02
B1-4	25%	19%	35%	0.02	29%	14%	45%	0.03	46%	31%	56%	0.02
B1-5	31%	23%	43%	0.02	27%	9%	44%	0.03	42%	27%	53%	0.03
B1-6	34%	26%	48%	0.02	43%	22%	66%	0.04	22%	1%	36%	0.03
B2-1	34%	26%	48%	0.02	50%	28%	71%	0.05	15%	0%	30%	0.04
B2-2	34%	26%	48%	0.02	50%	28%	70%	0.05	15%	0%	30%	0.04
B2-3	33%	25%	46%	0.02	30%	11%	49%	0.04	37%	19%	48%	0.03
B2-4	32%	24%	45%	0.02	24%	6%	42%	0.03	44%	28%	55%	0.03
B2-5	11%	8%	16%	0.01	42%	31%	58%	0.03	46%	31%	55%	0.03
B2-6	8%	6%	11%	0.01	46%	35%	62%	0.03	46%	30%	56%	0.03
B3-1	6%	5%	9%	0.00	48%	37%	65%	0.03	46%	29%	56%	0.03
B3-2	6%	5%	9%	0.00	48%	37%	65%	0.03	46%	29%	56%	0.03
B3-3	8%	6%	11%	0.01	49%	37%	66%	0.03	44%	27%	54%	0.03
B3-4	21%	16%	29%	0.01	33%	19%	48%	0.03	46%	32%	55%	0.02
B3-5	34%	26%	48%	0.02	21%	2%	39%	0.04	44%	29%	56%	0.03
B3-6	37%	28%	51%	0.02	53%	29%	70%	0.05	11%	0%	26%	0.04
B4-1	37%	28%	52%	0.02	29%	7%	49%	0.04	34%	16%	47%	0.03
B4-2	37%	28%	52%	0.02	29%	8%	50%	0.04	34%	15%	46%	0.03
B4-3	36%	27%	51%	0.02	22%	1%	40%	0.04	42%	26%	54%	0.03
B4-4	27%	20%	37%	0.02	27%	10%	42%	0.03	47%	32%	56%	0.02
B4-5	14%	10%	19%	0.01	45%	32%	61%	0.03	42%	26%	51%	0.03
B4-6	6%	5%	9%	0.00	49%	38%	67%	0.03	45%	27%	55%	0.03
B5-1	6%	4%	9%	0.00	49%	38%	67%	0.03	45%	28%	55%	0.03
B5-2	9%	7%	13%	0.01	50%	38%	68%	0.03	41%	24%	52%	0.03
B5-3	10%	8%	14%	0.01	48%	36%	66%	0.03	41%	24%	51%	0.03
B5-4	13%	10%	19%	0.01	45%	33%	62%	0.03	42%	25%	51%	0.03
B5-5	25%	19%	35%	0.02	28%	13%	44%	0.03	47%	32%	56%	0.02
B5-6	38%	28%	53%	0.02	48%	24%	68%	0.05	15%	0%	30%	0.04
E8-1	19%	14%	27%	0.01	38%	24%	54%	0.03	43%	28%	53%	0.03
E8-2	26%	19%	36%	0.02	37%	21%	56%	0.03	37%	20%	48%	0.03
E8-3	29%	22%	41%	0.02	40%	21%	60%	0.04	31%	12%	43%	0.03
E8-4	32%	24%	45%	0.02	41%	20%	62%	0.04	27%	7%	40%	0.03
E8-5	37%	28%	52%	0.02	56%	32%	70%	0.04	7%	0%	22%	0.04
E8-6	37%	28%	52%	0.02	56%	33%	71%	0.04	7%	0%	22%	0.03

C1-1	16%	12%	23%	0.01	38%	26%	53%	0.03	46%	32%	55%	0.02
C1-2	18%	14%	26%	0.01	37%	24%	52%	0.03	45%	30%	54%	0.02
C1-3	26%	19%	36%	0.02	34%	18%	52%	0.03	40%	24%	50%	0.03
C1-4	31%	23%	43%	0.02	30%	12%	48%	0.03	39%	23%	50%	0.03
C1-5	32%	24%	45%	0.02	34%	14%	54%	0.04	33%	15%	45%	0.03
C1-6	33%	25%	46%	0.02	42%	21%	64%	0.04	25%	5%	38%	0.03
C2-1	34%	26%	48%	0.02	51%	29%	72%	0.05	15%	0%	29%	0.04
C2-2	34%	26%	48%	0.02	53%	31%	72%	0.05	13%	0%	28%	0.04
C2-3	34%	25%	47%	0.02	35%	14%	55%	0.04	32%	13%	44%	0.03
C2-4	31%	24%	44%	0.02	29%	10%	48%	0.04	39%	23%	50%	0.03
C2-6	10%	7%	14%	0.01	44%	33%	60%	0.03	46%	30%	55%	0.03
C3-1	8%	6%	11%	0.01	48%	37%	66%	0.03	44%	27%	54%	0.03
C3-2	9%	7%	13%	0.01	47%	35%	64%	0.03	45%	28%	54%	0.03
C3-3	21%	16%	30%	0.01	33%	19%	48%	0.03	46%	32%	56%	0.02
C3-4	26%	20%	37%	0.02	28%	11%	44%	0.03	46%	31%	56%	0.02
C3-5	33%	25%	46%	0.02	30%	10%	48%	0.04	37%	20%	49%	0.03
C3-6	36%	27%	50%	0.02	46%	23%	68%	0.04	18%	0%	32%	0.04
C4-1	38%	28%	53%	0.02	30%	8%	50%	0.04	32%	14%	45%	0.03
C4-2	38%	29%	53%	0.03	28%	6%	48%	0.04	34%	16%	47%	0.03
C4-3	37%	28%	52%	0.02	22%	1%	41%	0.04	41%	24%	53%	0.03
C4-4	34%	25%	47%	0.02	21%	2%	38%	0.04	45%	30%	56%	0.03
C4-5	14%	11%	20%	0.01	42%	31%	58%	0.03	43%	28%	53%	0.03
C4-6	3%	2%	5%	0.00	49%	38%	66%	0.03	48%	32%	58%	0.03
C5-1	2%	1%	3%	0.00	41%	33%	56%	0.02	57%	43%	65%	0.02
C5-2	2%	1%	3%	0.00	42%	33%	57%	0.03	56%	42%	64%	0.02
C5-3	3%	2%	4%	0.00	48%	38%	65%	0.03	50%	33%	59%	0.03
C5-4	3%	2%	4%	0.00	50%	40%	68%	0.03	47%	30%	57%	0.03
C5-5	29%	22%	40%	0.02	24%	7%	40%	0.03	47%	33%	57%	0.02
C5-6	37%	28%	51%	0.02	40%	17%	62%	0.04	24%	3%	37%	0.03
C6-1	0%	0%	1%	0.00	10%	8%	13%	0.01	90%	87%	92%	0.01
C6-2	0%	0%	1%	0.00	10%	8%	13%	0.01	90%	87%	92%	0.01
C6-3	0%	0%	1%	0.00	11%	9%	15%	0.01	88%	84%	91%	0.01
C6-4	2%	1%	3%	0.00	43%	34%	58%	0.03	55%	41%	64%	0.02
C6-5	2%	1%	3%	0.00	62%	50%	85%	0.04	36%	15%	48%	0.04
C6-6	17%	13%	24%	0.01	61%	45%	83%	0.04	22%	1%	35%	0.04
E1-1	32%	24%	45%	0.02	32%	13%	52%	0.04	36%	18%	47%	0.03
E1-2	34%	25%	47%	0.02	34%	14%	54%	0.04	33%	14%	45%	0.03
E1-3	35%	27%	49%	0.02	36%	14%	57%	0.04	29%	10%	42%	0.03
E1-4	38%	28%	53%	0.02	36%	14%	58%	0.04	26%	6%	40%	0.03
E1-5	40%	30%	56%	0.03	38%	14%	61%	0.05	22%	1%	37%	0.04
E1-6	40%	30%	55%	0.03	38%	14%	61%	0.04	22%	1%	37%	0.03
D1-1	23%	17%	32%	0.02	33%	18%	49%	0.03	44%	29%	54%	0.02
D1-2	26%	20%	37%	0.02	32%	15%	49%	0.03	42%	26%	52%	0.03

D1-3	33%	25%	46%	0.02	32%	13%	52%	0.04	35%	17%	47%	0.03
D1-4	34%	26%	48%	0.02	34%	13%	54%	0.04	32%	13%	44%	0.03
D1-5	35%	26%	49%	0.02	47%	24%	69%	0.04	18%	0%	32%	0.04
D1-6	36%	28%	51%	0.02	60%	38%	72%	0.04	4%	0%	18%	0.03
D2-1	32%	24%	45%	0.02	57%	35%	74%	0.05	10%	0%	25%	0.04
D2-2	33%	24%	46%	0.02	51%	29%	72%	0.04	17%	0%	31%	0.04
D2-3	30%	23%	42%	0.02	36%	17%	55%	0.04	34%	16%	46%	0.03
D2-4	28%	21%	39%	0.02	33%	15%	50%	0.03	40%	23%	50%	0.03
D2-6	17%	13%	24%	0.01	37%	25%	53%	0.03	45%	31%	54%	0.02
D3-1	5%	4%	7%	0.00	49%	38%	66%	0.03	46%	29%	56%	0.03
D3-2	9%	7%	13%	0.01	47%	36%	64%	0.03	44%	27%	54%	0.03
D3-3	21%	16%	29%	0.01	32%	18%	47%	0.03	47%	32%	56%	0.02
D3-4	28%	21%	39%	0.02	27%	11%	44%	0.03	45%	30%	55%	0.02
D3-5	34%	26%	48%	0.02	23%	3%	40%	0.04	43%	28%	55%	0.03
D3-6	36%	27%	51%	0.02	56%	32%	71%	0.05	8%	0%	23%	0.04
D4-1	38%	29%	53%	0.02	44%	21%	66%	0.05	18%	0%	32%	0.04
D4-2	38%	28%	53%	0.02	37%	15%	60%	0.04	25%	4%	39%	0.03
D4-3	35%	27%	49%	0.02	24%	3%	42%	0.04	41%	25%	53%	0.03
D4-4	28%	21%	39%	0.02	26%	9%	42%	0.03	46%	31%	56%	0.02
D4-5	14%	11%	20%	0.01	42%	30%	58%	0.03	44%	29%	53%	0.03
D4-6	4%	3%	6%	0.00	50%	39%	68%	0.03	46%	29%	56%	0.03
D5-1	1%	1%	2%	0.00	28%	22%	37%	0.02	71%	62%	77%	0.02
D5-2	3%	2%	4%	0.00	49%	39%	67%	0.03	48%	31%	58%	0.03
D5-3	3%	2%	4%	0.00	52%	41%	70%	0.03	45%	28%	56%	0.03
D5-4	8%	6%	12%	0.01	50%	38%	68%	0.03	42%	25%	53%	0.03
D5-5	29%	22%	41%	0.02	21%	4%	36%	0.03	50%	37%	60%	0.02
D5-6	38%	28%	53%	0.02	49%	25%	69%	0.05	13%	0%	28%	0.04
D6-1	36%	27%	50%	0.02	32%	10%	52%	0.04	32%	14%	45%	0.03
D6-2	36%	27%	51%	0.02	31%	10%	52%	0.04	32%	14%	45%	0.03
D6-3	31%	24%	44%	0.02	32%	13%	51%	0.04	37%	20%	48%	0.03
D6-4	9%	7%	13%	0.01	52%	39%	70%	0.03	39%	21%	50%	0.03
D6-5	2%	1%	4%	0.00	47%	37%	64%	0.03	51%	34%	60%	0.03
D6-6	0%	0%	0%	0.00	10%	8%	13%	0.01	90%	87%	92%	0.01
D7-1	0%	0%	0%	0.00	4%	3%	6%	0.00	95%	94%	96%	0.00
D7-2	0%	0%	0%	0.00	6%	5%	8%	0.00	94%	92%	95%	0.00
D7-3	1%	0%	1%	0.00	27%	21%	36%	0.02	73%	63%	78%	0.02
D7-4	0%	0%	1%	0.00	69%	55%	89%	0.04	31%	11%	44%	0.04
D7-5	3%	2%	5%	0.00	60%	47%	81%	0.04	37%	17%	49%	0.03
D7-6	6%	4%	8%	0.00	72%	56%	95%	0.04	23%	0%	37%	0.04

Table S2. The mean, minimum, and maximum contribution values of different endmembers and standard deviation of each sample in NCS calculated by three-endmember mixing model.

Sample	CDW				SSW				SBW			
	mean	min	max	std	mean	min	max	std	mean	min	max	std
E10-1	1%	1%	2%	0.00	59%	48%	79%	0.03	39%	20%	51%	0.03
E10-2	1%	1%	2%	0.00	60%	48%	79%	0.03	39%	20%	51%	0.03
E10-3	2%	1%	3%	0.00	64%	51%	85%	0.03	34%	14%	47%	0.03
E10-4	2%	1%	4%	0.00	70%	56%	93%	0.04	28%	5%	41%	0.04
E10-5	2%	1%	4%	0.00	88%	70%	98%	0.04	10%	0%	27%	0.04
E10-6	3%	1%	4%	0.00	88%	71%	98%	0.04	10%	0%	26%	0.04
A1-1	1%	0%	2%	0.00	62%	50%	82%	0.03	37%	17%	49%	0.03
A1-2	1%	0%	2%	0.00	62%	50%	82%	0.03	37%	17%	49%	0.03
A1-3	1%	1%	2%	0.00	64%	52%	85%	0.03	34%	14%	47%	0.03
A1-4	1%	1%	2%	0.00	67%	54%	89%	0.04	32%	10%	45%	0.04
A1-5	2%	1%	3%	0.00	69%	55%	91%	0.04	30%	8%	43%	0.04
A1-6	2%	1%	3%	0.00	73%	58%	96%	0.04	25%	2%	40%	0.04
A2-1	4%	3%	6%	0.00	84%	67%	97%	0.04	12%	0%	29%	0.04
A2-2	4%	3%	6%	0.00	84%	67%	97%	0.04	12%	0%	29%	0.04
A2-3	4%	3%	6%	0.00	82%	66%	97%	0.04	14%	0%	30%	0.04
A2-4	2%	1%	3%	0.00	64%	51%	85%	0.03	34%	14%	47%	0.03
A2-5	1%	0%	2%	0.00	62%	50%	82%	0.03	37%	17%	49%	0.03
A2-6	1%	0%	2%	0.00	60%	48%	80%	0.03	39%	19%	50%	0.03
A3-1	1%	1%	2%	0.00	68%	54%	90%	0.04	31%	9%	44%	0.04
A3-2	1%	1%	2%	0.00	67%	54%	89%	0.04	31%	10%	44%	0.04
A3-3	1%	1%	2%	0.00	68%	54%	89%	0.04	31%	10%	44%	0.04
A3-4	3%	2%	5%	0.00	81%	65%	97%	0.04	15%	0%	31%	0.04
A3-5	4%	2%	5%	0.00	83%	66%	97%	0.04	14%	0%	30%	0.04
A3-6	4%	3%	6%	0.00	88%	71%	97%	0.04	8%	0%	25%	0.04
A4-1	3%	2%	5%	0.00	89%	72%	98%	0.04	7%	0%	24%	0.04
A4-2	3%	2%	5%	0.00	88%	70%	98%	0.04	9%	0%	26%	0.04
A4-3	3%	2%	5%	0.00	86%	69%	97%	0.04	10%	0%	27%	0.04
A4-4	3%	2%	5%	0.00	81%	64%	97%	0.04	16%	0%	32%	0.04
A4-5	1%	0%	2%	0.00	74%	60%	99%	0.04	24%	0%	39%	0.04
A4-6	1%	0%	2%	0.00	75%	60%	99%	0.04	24%	0%	39%	0.04
A5-1	1%	0%	2%	0.00	75%	60%	98%	0.04	23%	1%	38%	0.04
A5-2	1%	1%	2%	0.00	75%	60%	98%	0.04	23%	1%	38%	0.04
A5-3	1%	0%	2%	0.00	75%	60%	98%	0.04	23%	1%	38%	0.04
A5-4	2%	1%	3%	0.00	75%	60%	98%	0.04	23%	1%	38%	0.04
A5-5	3%	2%	4%	0.00	84%	67%	98%	0.04	13%	0%	30%	0.04

A5-6	2%	1%	4%	0.00	91%	74%	99%	0.04	7%	0%	23%	0.04
E9-1	2%	1%	3%	0.00	63%	50%	83%	0.03	36%	16%	48%	0.03
E9-2	2%	1%	3%	0.00	63%	50%	83%	0.03	36%	15%	48%	0.03
E9-3	2%	1%	3%	0.00	63%	51%	84%	0.03	35%	15%	47%	0.03
E9-4	2%	1%	3%	0.00	66%	53%	88%	0.04	32%	11%	45%	0.04
E9-5	2%	1%	4%	0.00	88%	71%	98%	0.04	9%	0%	26%	0.04
E9-6	3%	2%	4%	0.00	90%	72%	98%	0.04	8%	0%	25%	0.04
B1-1	2%	1%	3%	0.00	66%	53%	88%	0.04	32%	11%	45%	0.04
B1-2	2%	1%	3%	0.00	66%	53%	88%	0.04	32%	11%	45%	0.04
B1-3	2%	1%	3%	0.00	66%	53%	88%	0.04	32%	11%	45%	0.04
B1-4	2%	1%	3%	0.00	67%	53%	88%	0.04	32%	10%	45%	0.04
B1-5	2%	1%	3%	0.00	76%	61%	99%	0.04	23%	0%	37%	0.04
B1-6	3%	2%	4%	0.00	91%	75%	98%	0.03	6%	0%	22%	0.03
B2-1	2%	1%	3%	0.00	79%	63%	98%	0.04	19%	0%	34%	0.04
B2-2	2%	1%	3%	0.00	78%	62%	98%	0.04	20%	0%	35%	0.04
B2-3	2%	1%	3%	0.00	73%	58%	96%	0.04	26%	2%	40%	0.04
B2-4	2%	1%	3%	0.00	70%	56%	92%	0.04	29%	6%	42%	0.04
B2-6	1%	1%	2%	0.00	67%	54%	89%	0.04	32%	10%	45%	0.04
B3-1	2%	1%	3%	0.00	71%	57%	94%	0.04	28%	5%	42%	0.04
B3-2	2%	1%	2%	0.00	71%	57%	94%	0.04	27%	5%	41%	0.04
B3-3	2%	1%	2%	0.00	71%	57%	94%	0.04	27%	5%	41%	0.04
B3-4	2%	1%	3%	0.00	75%	60%	98%	0.04	23%	1%	38%	0.04
B3-5	2%	1%	4%	0.00	80%	64%	98%	0.04	17%	0%	33%	0.04
B3-6	3%	2%	4%	0.00	89%	71%	98%	0.04	9%	0%	26%	0.04
B4-1	3%	2%	4%	0.00	90%	73%	98%	0.04	7%	0%	24%	0.04
B4-2	3%	2%	4%	0.00	90%	73%	98%	0.04	7%	0%	23%	0.04
B4-3	3%	2%	5%	0.00	89%	72%	98%	0.04	8%	0%	25%	0.04
B4-4	3%	2%	5%	0.00	88%	71%	98%	0.04	9%	0%	26%	0.04
B4-5	2%	1%	3%	0.00	72%	58%	96%	0.04	26%	3%	40%	0.04
B4-6	2%	1%	3%	0.00	73%	58%	96%	0.04	26%	3%	40%	0.04
B5-1	2%	1%	3%	0.00	73%	58%	97%	0.04	25%	2%	40%	0.04
B5-2	2%	1%	3%	0.00	73%	58%	96%	0.04	26%	2%	40%	0.04
B5-3	2%	1%	3%	0.00	73%	58%	97%	0.04	26%	2%	40%	0.04
B5-4	2%	1%	3%	0.00	75%	60%	97%	0.04	24%	1%	38%	0.04
B5-5	3%	2%	4%	0.00	89%	71%	98%	0.04	9%	0%	25%	0.04
B5-6	3%	2%	4%	0.00	90%	73%	98%	0.04	7%	0%	24%	0.04
E8-1	2%	1%	3%	0.00	72%	57%	95%	0.04	26%	3%	40%	0.04
E8-2	2%	1%	3%	0.00	72%	57%	95%	0.04	26%	3%	40%	0.04
E8-3	2%	1%	4%	0.00	72%	58%	95%	0.04	26%	3%	40%	0.04
E8-4	2%	1%	4%	0.00	76%	61%	98%	0.04	21%	0%	36%	0.04
E8-5	3%	2%	4%	0.00	82%	65%	98%	0.04	16%	0%	32%	0.04
E8-6	3%	2%	5%	0.00	88%	70%	98%	0.04	9%	0%	26%	0.04
C1-1	2%	1%	3%	0.00	70%	56%	92%	0.04	28%	6%	42%	0.04

C1-2	2%	1%	3%	0.00	70%	56%	93%	0.04	27%	5%	41%	0.04
C1-3	2%	1%	3%	0.00	71%	57%	94%	0.04	27%	4%	41%	0.04
C1-4	2%	1%	3%	0.00	74%	60%	97%	0.04	23%	1%	38%	0.04
C1-5	2%	1%	3%	0.00	91%	74%	99%	0.04	7%	0%	24%	0.04
C1-6	2%	1%	4%	0.00	92%	75%	99%	0.04	6%	0%	23%	0.04
C2-1	2%	1%	3%	0.00	91%	74%	99%	0.04	7%	0%	24%	0.04
C2-2	2%	1%	3%	0.00	91%	74%	99%	0.04	7%	0%	23%	0.04
C2-3	2%	1%	4%	0.00	84%	67%	98%	0.04	14%	0%	30%	0.04
C2-4	2%	1%	3%	0.00	68%	54%	90%	0.04	30%	8%	43%	0.04
C2-6	2%	1%	3%	0.00	63%	50%	83%	0.03	35%	15%	48%	0.03
C3-1	2%	1%	3%	0.00	65%	52%	86%	0.03	33%	13%	46%	0.03
C3-2	2%	1%	3%	0.00	65%	52%	86%	0.03	33%	12%	46%	0.03
C3-3	2%	1%	3%	0.00	65%	52%	86%	0.03	33%	13%	46%	0.03
C3-4	2%	1%	3%	0.00	66%	53%	87%	0.04	32%	11%	45%	0.03
C3-5	2%	1%	3%	0.00	69%	55%	92%	0.04	29%	7%	42%	0.04
C3-6	3%	2%	4%	0.00	92%	76%	98%	0.03	5%	0%	21%	0.03
C4-1	2%	1%	4%	0.00	94%	78%	99%	0.03	4%	0%	19%	0.03
C4-2	2%	1%	4%	0.00	93%	77%	98%	0.03	5%	0%	20%	0.03
C4-3	2%	1%	4%	0.00	91%	73%	98%	0.04	7%	0%	24%	0.04
C4-4	3%	1%	4%	0.00	87%	70%	98%	0.04	10%	0%	27%	0.04
C4-5	1%	1%	2%	0.00	77%	61%	99%	0.04	22%	0%	37%	0.04
C4-6	1%	1%	2%	0.00	77%	61%	99%	0.04	22%	0%	37%	0.04
C5-1	1%	1%	3%	0.00	80%	64%	99%	0.04	19%	0%	34%	0.04
C5-2	1%	1%	2%	0.00	80%	64%	99%	0.04	19%	0%	34%	0.04
C5-3	1%	1%	2%	0.00	80%	64%	99%	0.04	19%	0%	34%	0.04
C5-4	1%	1%	3%	0.00	80%	64%	99%	0.04	19%	0%	34%	0.04
C5-5	3%	2%	5%	0.00	87%	70%	97%	0.04	10%	0%	26%	0.04
C5-6	4%	2%	5%	0.00	91%	74%	97%	0.03	5%	0%	22%	0.03
C6-1	3%	2%	4%	0.00	93%	78%	98%	0.03	4%	0%	19%	0.03
C6-2	3%	2%	4%	0.00	93%	78%	98%	0.03	4%	0%	19%	0.03
C6-3	3%	2%	4%	0.00	93%	78%	98%	0.03	4%	0%	19%	0.03
C6-4	3%	2%	4%	0.00	92%	75%	98%	0.03	5%	0%	21%	0.03
C6-5	2%	1%	3%	0.00	81%	65%	99%	0.04	17%	0%	33%	0.04
C6-6	1%	1%	2%	0.00	47%	38%	63%	0.03	51%	36%	61%	0.03
E1-1	4%	3%	6%	0.00	75%	60%	96%	0.04	21%	0%	36%	0.04
E1-2	4%	3%	6%	0.00	75%	60%	96%	0.04	21%	1%	36%	0.04
E1-3	4%	3%	6%	0.00	75%	60%	95%	0.04	20%	0%	35%	0.04
E1-4	6%	5%	9%	0.00	76%	60%	95%	0.04	18%	0%	33%	0.04
E1-5	8%	6%	11%	0.01	77%	61%	93%	0.04	15%	0%	31%	0.04
E1-6	8%	6%	11%	0.01	78%	61%	93%	0.04	14%	0%	30%	0.04
D1-1	3%	2%	4%	0.00	70%	56%	93%	0.04	27%	5%	41%	0.04
D1-2	3%	2%	4%	0.00	71%	57%	94%	0.04	26%	4%	40%	0.04
D1-3	3%	2%	5%	0.00	72%	58%	96%	0.04	24%	1%	39%	0.04

D1-4	3%	2%	5%	0.00	74%	59%	97%	0.04	22%	0%	37%	0.04
D1-5	4%	3%	5%	0.00	76%	61%	96%	0.04	20%	0%	35%	0.04
D1-6	5%	3%	6%	0.00	79%	63%	96%	0.04	17%	0%	32%	0.04
D2-1	4%	2%	5%	0.00	85%	68%	97%	0.04	12%	0%	28%	0.04
D2-2	4%	2%	5%	0.00	85%	68%	97%	0.04	12%	0%	28%	0.04
D2-3	3%	2%	4%	0.00	80%	64%	98%	0.04	18%	0%	33%	0.04
D2-4	2%	1%	3%	0.00	68%	55%	90%	0.04	30%	8%	43%	0.04
D2-6	2%	1%	3%	0.00	67%	53%	89%	0.04	31%	10%	44%	0.04
D3-1	2%	1%	3%	0.00	61%	49%	81%	0.03	37%	18%	49%	0.03
D3-2	2%	1%	2%	0.00	61%	49%	81%	0.03	37%	18%	49%	0.03
D3-3	2%	1%	2%	0.00	61%	49%	81%	0.03	37%	18%	49%	0.03
D3-4	2%	1%	3%	0.00	65%	52%	87%	0.03	33%	12%	45%	0.03
D3-5	2%	1%	3%	0.00	80%	64%	98%	0.04	18%	0%	33%	0.04
D3-6	2%	1%	4%	0.00	86%	69%	98%	0.04	11%	0%	28%	0.04
D4-1	3%	2%	4%	0.00	89%	72%	98%	0.04	8%	0%	25%	0.04
D4-2	3%	2%	4%	0.00	89%	72%	98%	0.04	8%	0%	25%	0.04
D4-3	3%	2%	4%	0.00	89%	72%	98%	0.04	8%	0%	25%	0.04
D4-4	2%	1%	3%	0.00	67%	54%	89%	0.04	31%	10%	44%	0.04
D4-5	2%	1%	3%	0.00	63%	51%	84%	0.03	35%	15%	47%	0.03
D4-6	2%	1%	3%	0.00	63%	50%	83%	0.03	36%	15%	48%	0.03
D5-1	1%	1%	2%	0.00	22%	18%	30%	0.01	77%	69%	81%	0.01
D5-2	1%	1%	2%	0.00	31%	25%	41%	0.02	68%	58%	74%	0.02
D5-3	2%	1%	3%	0.00	77%	62%	98%	0.04	21%	1%	36%	0.04
D5-4	2%	1%	3%	0.00	77%	62%	98%	0.04	21%	1%	36%	0.04
D5-5	2%	1%	4%	0.00	79%	64%	98%	0.04	18%	0%	34%	0.04
D5-6	3%	1%	4%	0.00	92%	75%	98%	0.03	6%	0%	22%	0.03
D6-1	3%	2%	4%	0.00	91%	74%	98%	0.04	6%	0%	23%	0.04
D6-2	3%	2%	4%	0.00	91%	74%	98%	0.04	6%	0%	23%	0.04
D6-3	3%	2%	4%	0.00	91%	74%	98%	0.04	6%	0%	23%	0.04
D6-4	3%	2%	4%	0.00	88%	71%	98%	0.04	9%	0%	26%	0.04
D6-5	2%	1%	3%	0.00	78%	62%	98%	0.04	21%	0%	36%	0.04
D6-6	1%	1%	1%	0.00	6%	5%	8%	0.00	93%	91%	95%	0.00
D7-2	1%	0%	1%	0.00	0%	1%	2%	0.01	98%	97%	98%	0.00
D7-3	2%	1%	3%	0.00	4%	61%	98%	0.75	23%	1%	37%	0.04
D7-4	2%	1%	3%	0.00	4%	61%	98%	0.76	22%	0%	37%	0.04
D7-5	2%	1%	3%	0.00	4%	63%	98%	0.78	20%	0%	35%	0.04
D7-6	3%	2%	5%	0.00	3%	76%	98%	0.92	5%	0%	21%	0.03